

# Benzothiazolyl and Benzoxazolyl Hydrazones Function as Zinc Metallochaperones to Reactivate Mutant p53

John A. Gilleran,<sup>¶</sup> Xin Yu,<sup>¶</sup> Alan J. Blayney,<sup>¶</sup> Anthony F. Bencivenga, Bing Na, David J. Augeri, Adam R. Blanden, S. David Kimball, Stewart N. Loh,<sup>&</sup> Jacques Y. Roberge,<sup>&</sup> and Darren R. Carpizo<sup>\*,&</sup>

**Cite This:** *J. Med. Chem.* 2021, 64, 2024–2045

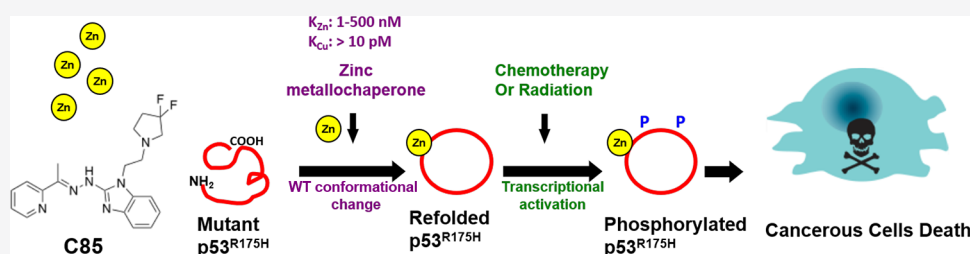
**Read Online**

ACCESS |

Metrics & More

Article Recommendations

Supporting Information



**ABSTRACT:** We identified a set of thiosemicarbazone (TSC) metal ion chelators that reactivate specific zinc-deficient p53 mutants using a mechanism called zinc metallochaperones (ZMCs) that restore zinc binding by shuttling zinc into cells. We defined biophysical and cellular assays necessary for structure–activity relationship studies using this mechanism. We investigated an alternative class of zinc scaffolds that differ from TSCs by substitution of the thiocarbamoyl moiety with benzothiazolyl, benzoxazolyl, and benzimidazolyl hydrazones. Members of this series bound zinc with similar affinity and functioned to reactivate mutant p53 comparable to the TSCs. Acute toxicity and efficacy assays in rodents demonstrated C1 to be significantly less toxic than the TSCs while demonstrating equivalent growth inhibition. We identified C85 as a ZMC with diminished copper binding that functions as a chemotherapy and radiation sensitizer. We conclude that the benzothiazolyl, benzoxazolyl, and benzimidazolyl hydrazones can function as ZMCs to reactivate mutant p53 *in vitro* and *in vivo*.

## INTRODUCTION

Mutant p53 remains one of the most significant targets in the field of cancer drug development for several reasons: (1) p53 is the most commonly mutated gene in human cancer; (2) the majority of mutations (>70%) are missense, leading to a single amino acid change that generates a defective protein found at higher levels in cancer cells (therefore being druggable); and (3) restoring wild-type p53 function in mouse cancer models is highly therapeutic. Small-molecule compounds that can restore the wild-type structure and function to these mutant p53s are often called mutant p53 reactivators. One recent and successful strategy to reactivate mutant p53 is using zinc metallochaperones (ZMCs).<sup>1,2</sup> The p53 protein requires the binding of a single zinc ion in order to facilitate proper folding. Experimentally, it has been shown that removing zinc will cause it to misfold and that by adding zinc back it will refold properly.<sup>3–5</sup> This inherent “malleability” of the protein is what allows the ZMC mechanism to function. A large number of mutations in p53 are located near the zinc coordination site and cause the protein to misfold by impairing zinc binding (reducing its  $K_d$  for zinc). The strong dependence of p53 protein folding on zinc binding serves as the basis for ZMC therapy. These compounds increase intracellular zinc, facilitating binding in the native zinc ligation site on the protein, which

then allows the protein to adopt a wild-type conformation. These zinc-deficient mutant p53s are best exemplified by the most common p53 missense mutant, p53<sup>R175H</sup>. We initially discovered a set of thiosemicarbazone (TSC) metal ion chelators that could reactivate zinc-deficient mutant p53s and elucidated their novel mechanism of action, which we termed “ZMCs”.<sup>6–8</sup> As ZMCs, these compounds bind extracellular zinc and function as zinc ionophores to raise intracellular zinc levels sufficiently to overcome the zinc-binding impairment induced by mutation in the p53 protein. This allows zinc to bind in its native p53 ligation site and induce a wild-type conformational change. We have validated this mechanism *in vivo* using genetically engineered murine models of cancer by showing that the lead TSC (ZMC1) has antitumor activity in mice harboring zinc-deficient p53 mutations while having no efficacy in mice with nonzinc-deficient p53 mutations.<sup>8–10</sup> We have also shown that we can

**Received:** September 8, 2020

**Published:** February 4, 2021



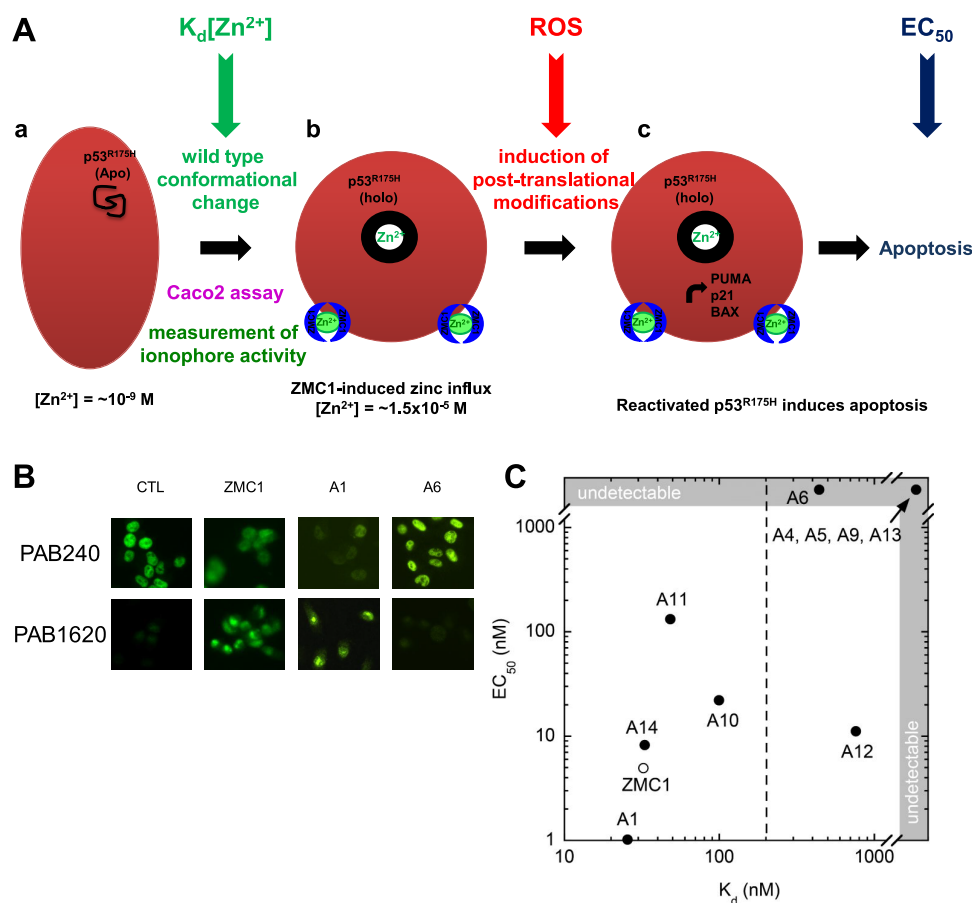


**Figure 1.** Development of a panel of assays for SAR.

improve efficacy in these models using a novel formulation of zinc-loaded ZMC1 in which we synthesized a 2:1 complex of ZMC1 and zinc.<sup>10</sup>

Our research thus far has demonstrated that the ZMC pathway represents a viable strategy for mutant p53-targeted anticancer drug development. One of the main objectives to move this field forward is to develop molecules with properties optimized for clinical development (solubility, potency, efficacy, and toxicity). The clinical utility of the class of thiosemicarbazones (TSCs) as anticancer drugs has been limited by toxicity and poor solubility.<sup>11,12</sup> The toxicity is thought to be attributed mainly to the chelation of redox-active metals such as iron.<sup>13</sup> Iron chelation has been shown to cause alternate mechanisms of toxicity including inhibition of ribonucleotide reductase (RR), the key iron-dependent enzyme that mediates the synthesis of deoxyribonucleotides, and methemoglobinemia.<sup>12</sup> Based on these limitations of TSCs, we sought to investigate an alternative zinc scaffold as potential clinical lead candidates that could perform this unique mechanism. Here, we designed and evaluated a new class of metal ion chelators (benzothiazolyl and benzoxazolyl hydrazones) with zinc-binding properties similar to TSCs that function as mutant p53 reactivators with better pharmacological properties. Given the novelty of the ZMC mechanism, we defined the assays required to conduct structure–activity relationship (SAR) studies and identified several candidate compounds, which were evaluated *in vitro* and *in vivo* preclinical studies. Lastly, we identified a new class of ZMCs with diminished copper-binding affinity that can function as

chemotherapy and radiation sensitizers to cancer cells harboring zinc-deficient p53 missense mutations.

## RESULTS AND DISCUSSION

**Unique Mechanism of Action Requires Development of Assays to Conduct SAR.** The delivery of a metal ion (like zinc) to restore the normal structure of a mutant protein is an entirely novel mechanism of action for a small-molecule drug. We further elucidated this novel mechanism to show that not only chaperoning of the metal ion through the plasma membrane was important (ionophore activity) but also increasing ROS levels was integral to its function<sup>6,14</sup> (Figure 1A). The ionophore activity ( $J_i$  drug/ $J_i$  DMSO) as  $-\log(\text{mol}/\text{m}^2\text{s})$  of the compounds is presented in Table 1 where a larger number indicates weaker ionophore activity. The major mechanism of regulation of p53 function is through post-translational modifications (PTMs) that not only guide which p53 targets are transcribed but also enhance or inhibit the transcription factor's ability to recruit the transcriptional machinery.<sup>15</sup> We demonstrated that the ZMC-induced ROS signal (likely through redox-active copper chelation) serves to induce the PTMs on p53 that typically results in an apoptotic program. In other words, without the ROS effect, a ZMC would induce a wild-type conformational change but would not induce an apoptotic program. To conduct SAR around this unique mechanism, we needed to first define the assays that would yield the necessary functional information to discriminate structural chemotype changes and second define the appropriate range in zinc binding for the small-molecule metal chelators that would induce conformational changes in p53.

Table 1. A- and C-Series Structure–Activity Exploration<sup>a,b</sup>

Structure	Code	Kd with RhodZin (nM)	Kd with FluoZin (nM)	EC <sub>50</sub> TOV-112D (μM)	EC <sub>50</sub> /ZMC1 EC <sub>50</sub>	Refolding p53 <sup>Δ125H</sup> – wild type	ROS (ROS/ZMC1 ROS)	Ionophore JI drug/JI DMSO -log[mol/m <sup>2</sup> ]	Caco-2 (5 μM) Papp (10 <sup>-6</sup> cm/s)	tPSA (calcd) Å <sup>2</sup>	ClogP (calcd)
	ZMC1 (NSC319726)	32.3 ± 2.2	28 ± 13	0.005	1	YES	1	12.4	15.6 ± 1.3	40	0.6
	A1	25.6 ± 0.7	NT	0.001	0.2	YES	1.3	12.8	7.3 ± 0.1	40	0.5
	A4	ND <sup>a</sup>	NT <sup>b</sup>	NT	NT	NO	NT	14.5	NT	64	1.9
	A5	ND	NT	NT	NT	NO	NT	12.4	NT	40	1.7
	A6	440 ± 18	NT	>10	NT	NO	0.9	12.9	NT	57	0.9
	A9	ND	NT	NT	NT	NO	0.9	11.6	NT	28	1.9
	A10	99.4 ± 4.6	NT	0.022	4.5	YES	2.0	11.8	NT	52	-0.5
	A11	48.3 ± 3.7	NT	0.132	26.7	YES	1.2	12.6	NT	10	1.1
	A12	760 ± 113	NT	0.011	2.3	NO	1.1	11.6	NT	40	1.1
	A13	ND	NT	NT	NT	NO	0.7	14.4	NT	40	1.8
	A14	33 ± 1.3	NT	0.008	1.7	NO	1.1	12.5	NT	43	1.3
Structure	Code	Kd with RhodZin (nM)	Kd with FluoZin (nM)	EC <sub>50</sub> TOV-112D (μM)	EC <sub>50</sub> /ZMC1 EC <sub>50</sub>	Refolding p53 <sup>Δ125H</sup> – wild type	ROS (ROS/ZMC1 ROS)	Ionophore JI drug/JI DMSO -log[mol/m <sup>2</sup> ]	Caco-2 (5 μM) Papp (10 <sup>-6</sup> cm/s)	tPSA (calcd) Å <sup>2</sup>	ClogP (calcd)
	C1	141 ± 7	119 ± 8	0.055	11.16	YES	1.7	11.6	4.4 ± 0.1	49	2.7
	C2	90 ± 14.5	77 ± 20	0.006	1.25	YES	1.5	11.8	10.6 ± 0.5	58	2.0
	C9	171 ± 24	63 ± 17	0.004	0.74	YES	1.1	11.6	NT	52	2.1
	C21	193 ± 22	192 ± 27	0.048	5.9	YES	1.2	11.6	NT	52	3.4
	C22	298 ± 20	44 ± 15	0.141	17.6	YES	2.2	11.6	NT	49	2.6
	C23	386 ± 6	81 ± 17	NT	NT	YES	2.4	11.6	NT	68	2.9
	C27	NT	61 ± 21	0.042	5.2	YES	1.6	11.6	NT	56	2.3
	C28	NT	55 ± 19	NT	NT	YES	2.5	11.6	NT	62	3.2
	C35	NT	47 ± 16	0.053	5.6	YES	1.4	12.2	NT	71	2.5
	C42	NT	71 ± 23	0.051	5.4	YES	1.0	11.6	NT	65	2.1
Structure	Code	Kd with RhodZin (nM)	Kd with FluoZin (nM)	EC <sub>50</sub> TOV-112D (μM)	EC <sub>50</sub> /ZMC1 EC <sub>50</sub>	Refolding p53 <sup>Δ125H</sup> – wild type	ROS (ROS/ZMC1 ROS)	Ionophore JI drug/JI DMSO -log[mol/m <sup>2</sup> ]	Caco-2 (5 μM) Papp (10 <sup>-6</sup> cm/s)	tPSA (calcd) Å <sup>2</sup>	ClogP (calcd)
	C61	NT	22 ± 2	NT	NT	NO	2.8	11.6	NT	79	2.2
	C64	NT	20 ± 5	NT	NT	NO	0.9	11.6	NT	65	2.3
	C65	NT	197 ± 16	NT	NT	YES	0.9	11.6	NT	58	2.3
	C69	NT	22 ± 5	0.093	9.9	YES	1.2	11.6	NT	56	2.8
	C77	NT	79 ± 3	NT	NT	NO	1.2	11.8	NT	61	1.7
	C78	NT	408 ± 18	0.445	47.1	YES	0.9	11.8	NT	52	0.5
	C85	NT	26 ± 3	0.151	31	YES	0.8	12.2	NT	56	3.1
	C89	NT	54 ± 1	NT	NT	NO	1.6	12.0	NT	65	1.2

<sup>a</sup>ND, not detected. <sup>b</sup>NT, not tested.

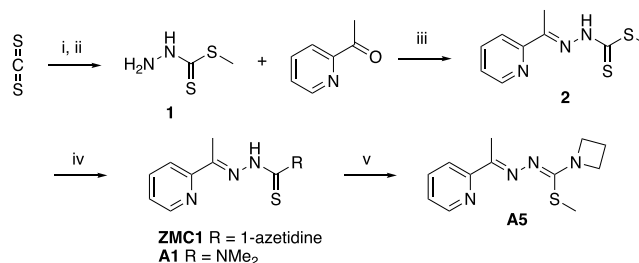
These compounds are intermediate strength chelators such that their affinity for zinc is tight enough to steal zinc from

serum albumin ( $K_{Zn} \approx 100$  nM), which is the major source of available zinc in the blood, but weak enough to donate it to

mutant p53 ( $K_{Zn} \approx 0.01$ – $100$  pM).<sup>16–19</sup> We previously determined the ZMC1  $K_{Zn}$  to be 30 nM, but the range of zinc affinity sufficient for zinc metallochaperone function was unclear. To investigate this, we performed a rigorous study of a small set of ZMC1 derivatives, using the following assays to guide synthesis: (1)  $K_{Zn}$  *in vitro*, (2)  $EC_{50}$  in p53<sup>R175H</sup> expressing cancer cells, (3) cellular immunofluorescence using p53 conformation-specific antibodies to monitor conformational change (PAB1620 for wild type and PAB240 for mutant conformation) (Figure 1B), (4) ROS change by flow cytometry analysis using a fluorescent probe, and (5) membrane permeability using Caco-2 assays. We first validated the SAR assays of ZMC1 and its analogues (A1 and A6, Table 1)<sup>14</sup> and found that for SAR, the most useful assays were (1) zinc affinity ( $K_{Zn}$ ), (2)  $EC_{50}$  for a p53<sup>R175H</sup> cell line, and (3) evidence of conformational change (refolding). We reasoned that the  $EC_{50}$  was a reasonable indicator of the ionophore activity as any change that impaired the compound's ability to traverse the plasma membrane would negatively affect its  $EC_{50}$ ; moreover, any change that limited the ROS level would also limit its transcriptional activity and hence its efficacy in inducing an apoptotic program. We next evaluated a number of structural modifications that we thought would significantly impact zinc binding in a focused SAR study (Table 1; molecular changes are highlighted). All the compounds in Table 1 are new except for ZMC1, Zn-1,<sup>6</sup> and A6.<sup>14</sup> We found, for the most part, that all structures that bound zinc with  $K_{Zn} < 200$  nM (A1, ZMC1, A10, and A11) induced a wild-type conformational change and prompted cell killing at a level similar to or greater than ZMC1. The exception was A14, which did not induce a conformational change yet maintained significant cytotoxicity against the mutant p53 cell line. Later results suggested that A14 induced cell death through an alternate mechanism likely through the chelation of redox-active metals such as copper.<sup>20</sup> Likewise, compounds with a  $K_{Zn} > 200$  nM (A4, 5, 6, 9, 12, and 13) could no longer induce a conformational change and were consequently not cytotoxic with the exception of A12. The effective upper limit of  $K_{Zn}$  is set by the dissociation constant of serum albumin for  $Zn^{2+}$  ( $\sim 100$  nM) and is thus likely to be similar for all zinc metallochaperones. The observed cutoff of  $K_{Zn} \approx 200$  nM is expected as compounds with larger  $K_{Zn}$  values bind zinc too weakly to compete with BSA in our assays. These results, illustrated in Figure 1C, indicate that we have defined an upper limit for the optimal  $K_{Zn}$  range for a zinc metallochaperone at approximately 200 nM. Although there were exceptions, we could use this number as a cutoff point to save resources. In terms of SAR, we found that replacing the thiourea moiety with a urea (A6), blocking the thiol via alkylation with a methyl (A5), or replacing the pyridine with a phenyl (A9) increased the  $K_{Zn}$  to  $>400$  nM. This resulted in a subsequent loss of its ability to induce a conformational change in p53 and hence its activity as a cytotoxic agent (Table 1 and Figure 1C). Replacement of the pyridine with the much less basic piperazine<sup>21</sup> (A10) and methylation at C-6 of the pyridine (A11) were both tolerated. Replacement of the azetidine or dimethylamine with substituted aminopiperazine (A4) and addition of bulky groups that would likely reduce zinc binding (A12 and A13) prevented the refolding of p53.

**Synthesis of A-Series Compounds.** ZMC1 and A1 were prepared by displacing the methylthiol of intermediate 2, and A5 was obtained via S-methylation of ZMC1 (Scheme 1). The thiocarbonyl in compounds A4 and A9–A14 is introduced

**Scheme 1.** (i) KOH,  $N_2H_4 \cdot H_2O$ , *i*-PrOH, and  $H_2O$ ; (ii) MeI; (iii) EtOH; (iv) Azetidine or Dimethylamine and EtOH; and (v) ZMC1, MeI, EtOH, and DCM



with *N,N*-diimidazothiocarbonyl and hydrazine followed by the displacement of the remaining imidazole with the selected amine (Scheme 2). The resulting hydrazinocarbothioamides are coupled with ketones to give the thiosemicarbazones.

The carbonyl analogue of A6 was prepared via addition of azetidine to the nitrophenoxycylated 2-acetylpyridine hydrazone (Scheme 3).

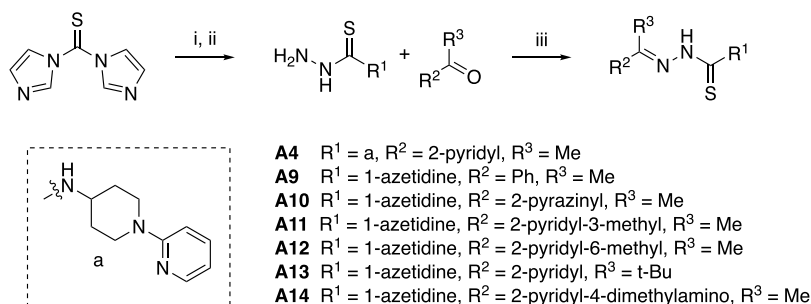
**Benzothiazolyl and Benzoxazolyl Hydrazones: An Alternative ZMC.** To identify a nonthiosemicarbazone ZMC, we turned to another class of zinc chelators (benzothiazolyl C1 and benzoxazolyl hydrazones C2 (Figure 2B)), which were designed with the goals of decreasing off-target toxicity and increasing potency over the TSCs.<sup>22</sup>  $\alpha$ -(*N*)-Heteroaromatic TSCs (i.e., ZMC1) have a characteristic N–NH–C–S backbone, while the benzothiazolyl, benzoxazolyl, and benzimidazolyl (C9) hydrazones would be expected to have a N–NH–C–N backbone with the last nitrogen mimicking the thiocarbonyl. This is demonstrated through the crystal structure determination shown in Figure 2.  $pK_a$  calculations<sup>23</sup> of the NH for TSCs ( $\sim 11.8$ ) showed that they are in a range similar to the benzimidazole ( $\sim 13.7$ ) but different from the more acidic benzothiazoles (7–9) and benzoxazoles ( $\sim 7$ ). Aside from toxicity due to copper or iron chelation, it was thought that part of the toxicity of the TSCs is related to the release of  $H_2S$  during metabolism.<sup>24</sup> In fact, structure–activity relationship (SAR) studies in which the thiocarbamoyl structure was replaced by a 2-pyridinyl moiety showed a drastic reduction in toxicity and retention of biological activity.<sup>25</sup> The general design principle behind this class of chelators is similar in that the thiocarbamoyl moiety is replaced by a benzothiazole or benzoxazolyl.<sup>22</sup> The two scaffolds have very similar interatomic spacing and binding elements that allow for nearly equivalent zinc-binding affinities. Studies on these compounds in cancer cells revealed increased potency over TSCs, but interestingly, they did not inhibit RR, and thus, their exact mode of action is currently still unknown.<sup>26</sup>

**Synthesis of C-Series Compounds.** Selective alkylation of 2-aminobenzo[d]thiazol-6-ol followed by substitution of the amino group with hydrazine provided the substituted hydrazine intermediate 9 (Scheme 4). The benzimidazole intermediates 11 and 15 are prepared by NH alkylation using sodium hydride on 2-chlorobenzimidazole and then displacement of the chloride with hydrazine.

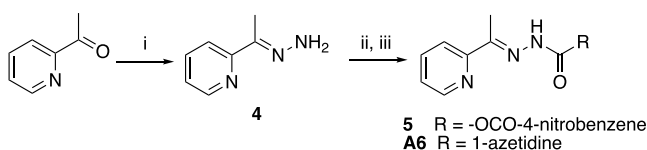
The 4-*O*-alkylated-2-acetylpyridine was prepared in a straightforward fashion according to Scheme 5.  $S_NAr$  on 4-chloro-2-cyanopyridine gave dimethylamine 12 and THP-protected ether 16. Both were subjected to the methylmagnesium iodide addition and hydrolysis. Compound 12 gave the desired ketone 13, while the ketone derived from 16 was



Scheme 2. (i) TEA and THF; (ii)  $\text{N}_2\text{H}_4\cdot\text{H}_2\text{O}$  and EtOH; and (iii) DCM and  $\text{AcOH}_{(\text{cat.})}$



Scheme 3. (i)  $\text{N}_2\text{H}_4\cdot\text{H}_2\text{O}$  and EtOH; (ii) 4-Nitrophenyl Carbonochloridate and DCM; and (iii) Azetidine, TEA, and DCM



further hydrolyzed to give alcohol 17. 17 was mesylated, and the mesylate 18 was displaced with 4-methylpiperazine to give 19.

The synthesis of C65 is shown in Scheme 6, where the bromoacetylpyridine is simultaneously methoxylated while the hydrazone is formed.

The majority of the hydrazone preparations were done in methanol with acetic acid or with additional hydrochloric acid to give the HCl salt, as shown in Scheme 7.

The syntheses of the substituted azole analogues (C69, C78, C85, and C89) are shown in Scheme 8. Alkylation of benzimidazoles (21 and 25) is followed by lithiation and addition to di-*tert*-butyl-azodicarboxylate, providing the di-Boc-substituted hydrazines (22, 26, and 27). Simultaneous hydrazine deprotection and condensation with the appropriate ketone provided the desired products.

Heterocycles such as benzothiazole C1, benzoxazole C2, and *N*-methylbenzimidazole C9 contain a  $\text{C}=\text{N}$  double bond and an acidic NH that once deprotonated functions to coordinate  $\text{Zn}^{2+}$  ions analogously to that of the  $\text{C}-\text{S}$  thiolate of a thiosemicarbazone (Figure 2A). We resolved the X-ray crystal

structure of C1 in complex with zinc and found it to bind as a 2:1 octahedral complex with zinc (Zn-2, Figure 2B), just as had been previously published for ZMC1<sup>6</sup> (Zn-1, Figure 2B). Furthermore, the internal carbonyl  $\text{C}=\text{N}$  coordinates zinc in this 2:1 complex analogously to the  $\text{C}-\text{S}$  of ZMC1 with  $\text{S}-\text{Zn}$  being slightly longer than  $\text{N}-\text{Zn}$  of the benzothiazole in the crystal structures (2.45 and 2.10 Å, respectively, see Scheme 9). The two hydrazinyl moieties of the ligands are each deprotonated and each bear one negative charge that balances the  $\text{Zn}^{2+}$  ion charge. The remaining pyridine and benzothiazole rings contain  $\text{C}=\text{N}$ : nitrogen atoms with a nitrogen lone pair available for d-orbital insertion. This neutral complex is then capable of ionophore activity to traverse the plasma membrane of the cell to deliver zinc intracellularly. Donation of zinc within the cell is followed by tetrahedral coordination with key Cys176–His179 of L2 and Cys238–Cys242 of L3 residues on mutant p53.<sup>1</sup> The tetracoordinated residues then trigger a wild-type conformational change that leads to a p53-mediated apoptotic cellular death. We tested C1 and C2 for their affinity for zinc as well as in cell growth inhibition assays using ZMC1 as a control. We found the  $K_{\text{Zn}}$  for C1 and C2 to be 141 and 90 nM, respectively, which is within the range of the  $K_{\text{Zn}}$  we determined in Table 1. Both C1 and C2 showed toxicity for the p53<sup>R175H</sup> mutants with similar potency to ZMC1 (Table 1) and exhibited allele selectivity as they demonstrated almost no cell kill in the p53 wild type and p53 null cell lines (Suppl. Figure S1). Furthermore, we found that they both induced a wild-type conformational change in the p53<sup>R175H</sup> (Table 1). Taking all three factors into account, we concluded that both C1 and C2 function as zinc metallochaperones *in vitro*.

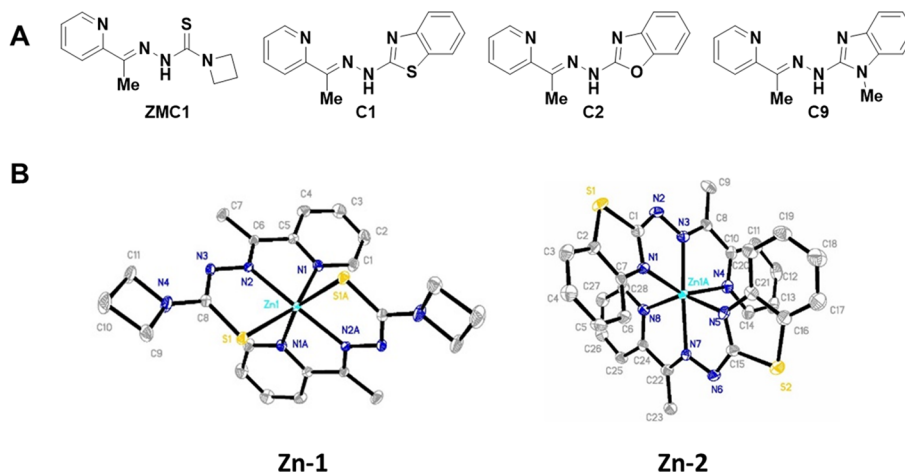
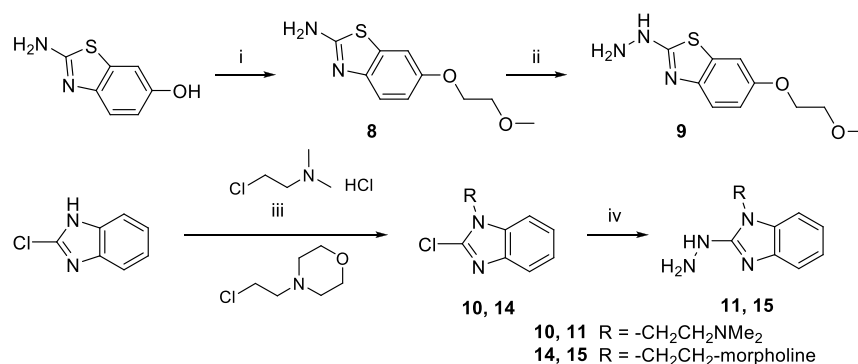
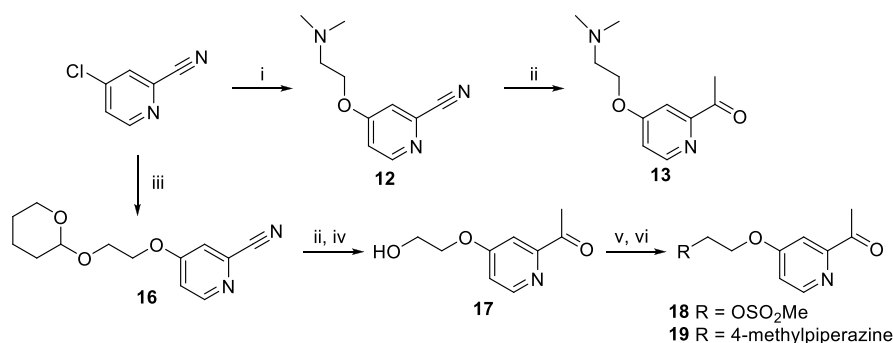


Figure 2. (A) Simplest C-series analogues of ZMC1. (B) X-ray structures of Zn-1 and Zn-2.

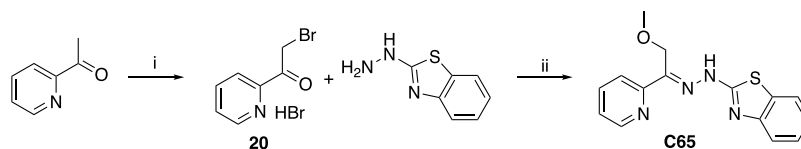
**Scheme 4.** (i) 1-Bromo-2-methoxyethane,  $\text{Cs}_2\text{CO}_3$ , and DMF; (ii)  $\text{N}_2\text{H}_4 \cdot \text{H}_2\text{O}$ , HCl (Concd), and Ethylene Glycol; (iii) NaH and DMF; and (iv)  $\text{N}_2\text{H}_4 \cdot \text{H}_2\text{O}$ , *i*-PrOH, or Ethylene Glycol



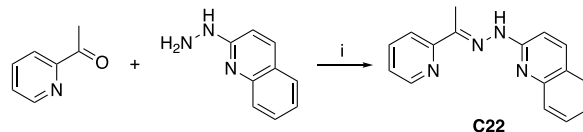
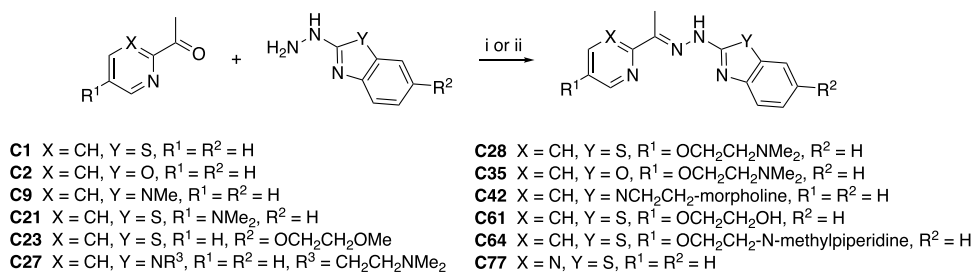
**Scheme 5.** (i) 2-(Dimethylamino)ethan-1-ol, NaH, and DMF; (ii) MeMgI (3 M/ $\text{Et}_2\text{O}$ ) and THF; (iii) 2-((Tetrahydro-2H-pyran-2-yl)oxy)ethan-1-ol, NaH, and DMF; (iv) HCl; (v) MsCl, TEA, and DCM; and (vi) 1-methylpiperazine, KI,  $\text{K}_2\text{CO}_3$ , and MeCN



**Scheme 6.** (i) HBr,  $\text{Br}_2$ , and AcOH and (ii) AcOH and DCM/MeOH



**Scheme 7.** (i) MeOH and  $\text{AcOH}_{(\text{cat.})}$  and (ii) MeOH and  $\text{AcOH}_{(\text{cat.})}$  followed by 4 M HCl/dioxane

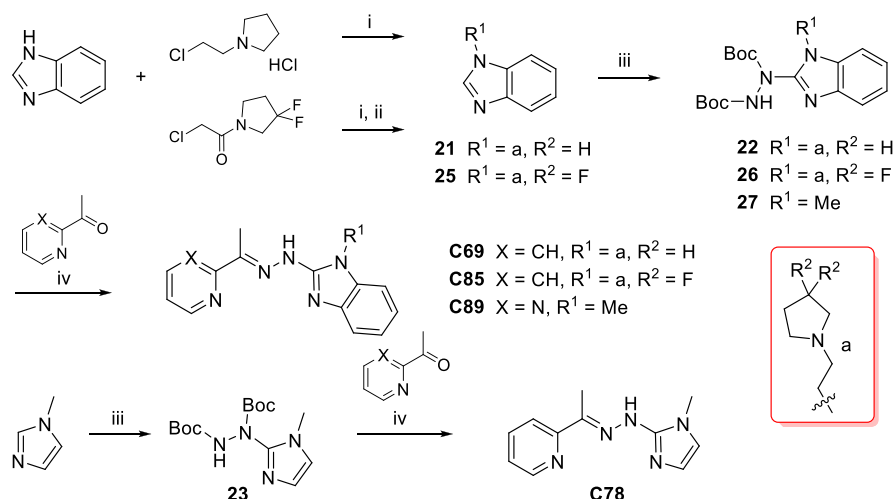


**Synthesis of Zn-1 and Zn-2.** The zinc complexes Zn-1 and Zn-2 are prepared by heating in the presence of triethylamine and zinc chloride in ethanol followed by recrystallization (Scheme 9).

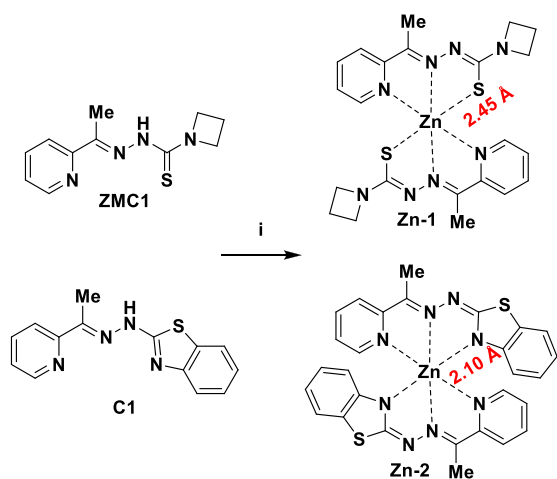
**C-Series Evolution.** The evolution of the C-series is shown in Figure 3. Replacement of the hydrazinothiocarbonyl of

ZMC1 by hydrazinobenzoic heterocycles led to C1 (benzothiazole), C2 (benzoxazole), and C9 (benzimidazole), which maintained activity but suffered from low aqueous solubility.<sup>27</sup> Addition of solubilizing polyethers (C23) or alkylamines (C27 and C28) resulted in more soluble compounds with better physical properties. Further optimization of the solubilizing

Scheme 8. (i)  $K_2CO_3$  and DMF; (ii)  $BH_3 \cdot THF$  and THF; (iii) Di-*tert*-butyl-azodicarboxylate, *n*-BuLi (2.5 M in Hexanes), and THF; and (iv) MeOH, 4 M HCl/Dioxane (Excess)



Scheme 9. (i)  $ZnCl_2$ , TEA, and EtOH



amines led to compounds like C35, C42, and C69, which had a mixture of cellular activity and physical properties that made them attractive to pursue further. Evaluation in the CEREP44 safety screen<sup>28</sup> showed ion channel liabilities with the most serious one being the potassium channel hERG (from human ether-à-go-go-related gene) due to its known association with serious cardiovascular risks (Table 2). Conversion of the benzimidazole substituent of C9 to an imidazole (C78) resulted in a compound with a decreased 1-octanol/water partition coefficient (ClogP).<sup>29</sup> In addition, the removal of one of the lipophilic bases of the triangular hERG pharmacophore resulted in a compound devoid of liabilities observed in the CEREP screen results of earlier analogues.

The 2-quinolinyl heterocycle C22 possesses a polarized internal carbonyl mimic in the form of the quinoline nitrogen that binds the zinc ion tightly, probably the consequence of six-membered ring geometry, with a  $K_{Zn}$  of 44 nM. However, it was not as effective as C9 against TOV-112D cells (Table 1). The dimethylaminoethoxy substituent appended to the pyridine ring of C35 proved to be a solubilizing group with

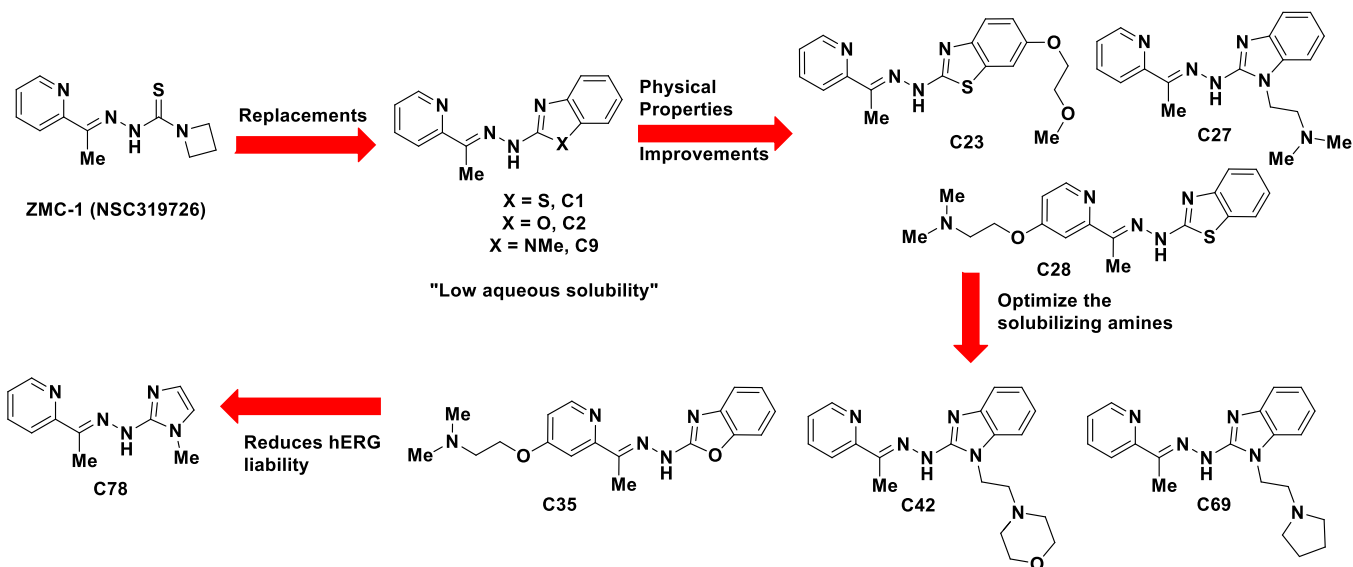
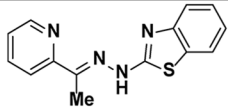
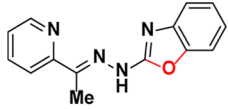
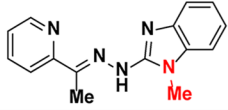
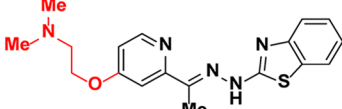
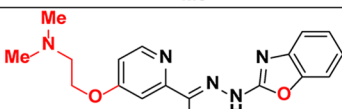
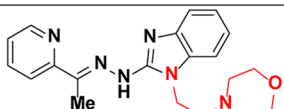
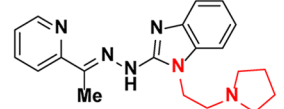
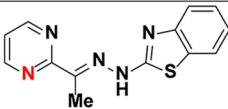
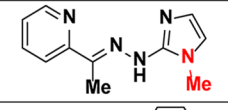
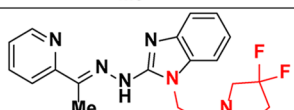
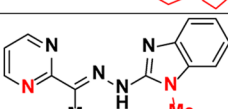


Figure 3. Evolution of the C-series.

Table 2. CEREP Safety Screening Selected Results

Structure	#	Kd with FluoZin (nM)	Human $\mu$ -Opiate Rec. (OP3) %Inh.@10 $\mu$ M	Human hERG [ $^3$ H]-Dofetilide %Inh.@10 $\mu$ M	Human Serotonin 5-HT <sub>2A</sub> %Inh.@10 $\mu$ M	Rat Sodium Channel site 2 %Inh.@10 $\mu$ M	Human Norepinephrine Transporter %Inh.@10 $\mu$ M	tPSA (calcd) Å <sup>2</sup>	ClogP (calcd)
	C1	119	13	19	96	101	101	49	2.7
	C2	77	2	21	-4	12	21	58	2.0
	C9	63	48	86	46	7	61	52	2.1
	C28	55	48	95	76	36	82	62	3.2
	C35	47	0	51	32	21	-25	71	2.5
	C42	71	9	76	100	50	-7	65	2.1
	C69	22	78	88	96	101	101	56	2.8
	C77	71	4	-2	3	2	84	61	1.7
	C78	408	-2	7	11	23	4	52	0.5
	C85	26	88	101	92	88	-1	56	3.1
	C89	54	41	77	11	12	-2	65	1.2

a favorable topological polar surface area (tPSA)<sup>30</sup> and CLogP, subsequently leading to mutant p53 protein refolding (the tPSA and cLogP were calculated using ChemDraw or MOE). tPSA is also an accurate predictor of permeability and drug absorption as well as a predictor of absorption across the blood–brain barrier (BBB).<sup>31</sup> In addition, the alkoxy group at the 4-position of C35 increased the electron density on the pyridine nitrogen helping to tune the Zn/Cu binding ratio. This effect was also observed with the dimethylamino substituent on A14, but unlike in the case for C35, it did

not lead to mutant p53 refolding. However, C21 was able to refold p53 even though the zinc-binding affinity was the borderline. Morpholine, another widely used solubilizing group,<sup>32</sup> can be tethered to the benzimidazole nitrogen as seen in *N*-ethylmorpholino analogue C42. Functionalized pyrrolidines (C69 and C85) can also be used as solubilizing side chains and do not appear to interfere with complex formation or dissociation. The benzothiazolyl C61 (Table 1) utilizes a hydroxyethyl appendage to increase solubility, which could possibly prevent hERG channel inhibition. The



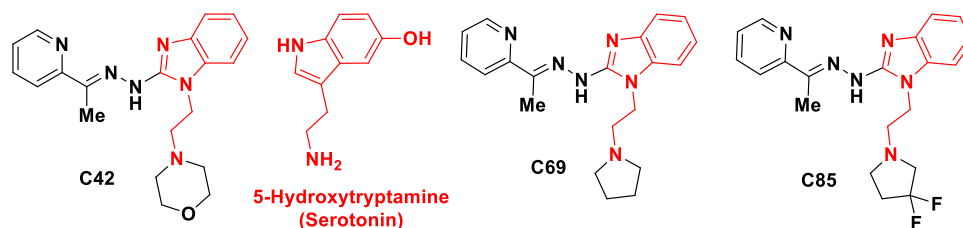


Figure 4. C-Series compound structures compared with that of serotonin.

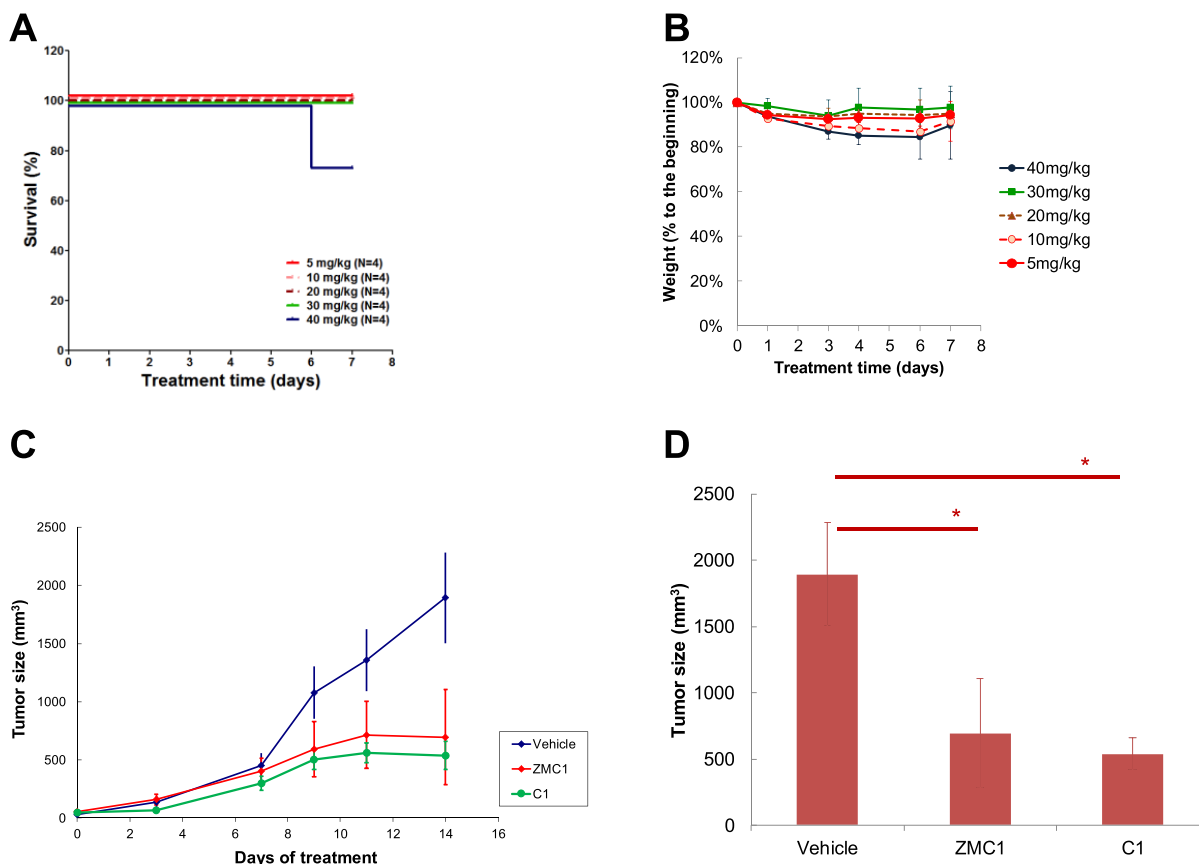


Figure 5. Efficacy of C1.

structural elements most commonly associated with this hERG liability are the presence of a basic amine ( $pK_a > 7.3$ ), lipophilicity ( $ClogP > 3.7$ ), a lack of negatively ionizable groups, and a lack of oxygen H-bond acceptors. Potassium hERG channel inhibitors often have a triangular or pyramidal pharmacophore with a basic group at the apex and two (or three) lipophilic groups at the base. These inhibitors are thought to act as a plug for the channel.<sup>33</sup> A range of solubilizing functional groups were appended to either the 4-position of the pyridine ring or to the free NH of the benzimidazole ring, in search of improved solubility. C61 showed good characteristics and an acceptable zinc  $K_d$  but did not initiate mutant protein refolding (Table 1). The *N*-methyl-piperizinyethyl analogue C64 showed good zinc binding but was also unable to demonstrate protein refolding. C69 was able to demonstrate protein refolding. In addition, it had a favorable tPSA and ClogP as well as a good balance between aliphatic and aromatic character and thus was advanced for further studies. Many of the Table 1 analogues possess favorable absorption and permeability characteristics but were not active

in protein refolding and were excluded from further consideration.

A standard CEREP safety panel was used to determine the level of inhibition of most of the ion channels, CNS receptors, and hERG (Table 2). The results of the screen indicated that this particular class of chelating ligands inhibits 5-hydroxytryptamine (SHT, serotonin) receptors, opiate  $\mu$  receptors, hERG,  $Na^+$  channel, and even the norepinephrine transporter. It is evident that two of the C-series benzimidazole analogues, C42 and C69, overlay quite well with SHT, hence the 100 and 95% inhibition of the serotonin SHT receptor, respectively (Figure 4). Many of the compounds in this series are active against targets one wishes to avoid. Besides the SHT receptor activity that were observed for C42 and C69, structures with a 2-carbon tether to a basic amine, C9, C28, C42, C69, and C89 all showed strong hERG inhibition at 10  $\mu M$ . Several compounds showed activity against the sodium channel (C1 and C69) and the norepinephrine transporter (C1, C28, C69, and C77). An ethyl-3,3-difluoropyrrolidine ring was added to the benzimidazole core to generate C85, reducing the calculated  $pK_b$  of the side chain's basic nitrogen by more

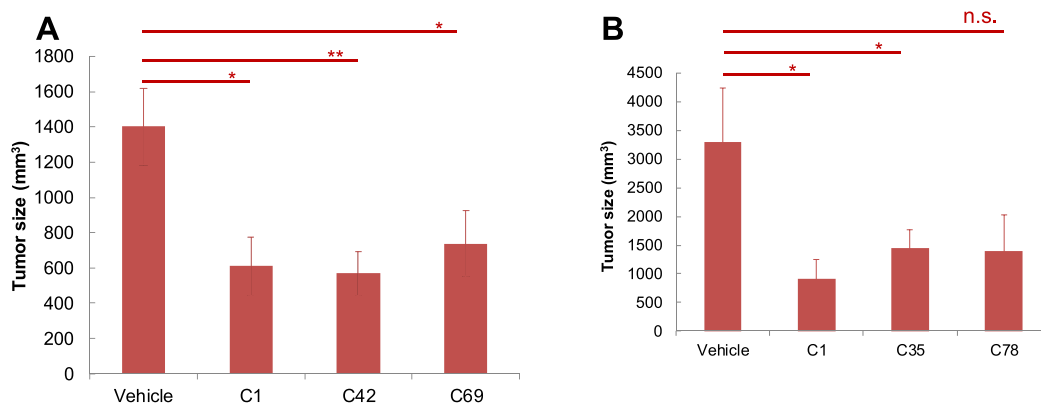


Figure 6. Efficacy of the other C compounds.

than 3.2 units to 5.9 as compared to C69 possibly eliminating the hERG liability and the hydroxytryptamine mimicry.<sup>23</sup> Recent CEREP44 screening results however did not support the increased acidity hypothesis, with the compound showing potent hERG inhibition as well as other liabilities (Table 2).

**Benzothiazolyl Hydrazones Function as Zinc Metallochaperones *In Vivo*.** To further evaluate the potential of these compounds for clinical development as zinc metallochaperones, we studied C1 for toxicity and efficacy in mice. We first determined the maximum tolerated dose (MTD) using acute single-dose exposure toxicity assays for each selected compound that previously showed low EC<sub>50</sub> values and reactivation of p53 functions in the cellular assays. Then, we treated the animals bearing the p53<sup>R175H</sup> mutant tumors with these compounds to compare the efficacy. We found that C1 was well tolerated up to 30 mg/kg without significant weight loss, much better than ZMC1 where the MTD was 5 mg/kg<sup>10</sup> (Figure 5A,B). This indicated that the benzothiazolyl hydrazones are indeed less toxic than the TSCs. To compare the efficacy of C1 and ZMC1 at 5 mg/kg (a dose which we know is effective *in vivo* for ZMC1), we dosed the molar equivalent of C1 (5.73 mg/kg). We found that, like ZMC1 (which reduced tumor growth by 63%), C1 treatment also significantly inhibited the tumor growth (reduced tumor growth by 72%), implying that C1 could be used to reactivate p53<sup>R175H</sup> mutation *in vivo* (Figure 5C,D). We also observed that like ZMC1, the tumor growth inhibition by C1 was allele specific in that C1 did not inhibit the tumor growth derived from p53<sup>R273H</sup>, which is not a Zn-deficient mutation (Suppl. Figure S2).

We then carried out the *in vivo* efficacy studies for several candidate compounds selected from the cellular assays. We confirmed that the doses were not toxic to the normal mice by the MTD assay (Suppl. Figure S3). Then, we treated the p53<sup>R175H</sup> tumors with compounds C42 and C69 (Figure 6A) and C35 and C78 (Figure 6B), in comparison to C1. The studies showed similar efficacy between these compounds over a 15 day trial with significant tumor growth inhibition (reduced tumor growth: C42, 59%; C69, 47%; C35, 56%; and C78, 57%) (Figure 6 and Suppl. Figure S3).

**C-Series Compounds that Function as a New Class of Zinc Metallochaperones: Chemotherapy/Radiation Sensitizers.** Systemic chemotherapy and radiation have previously been shown to be more effective in tumors with wild-type p53 as these therapies activate wild-type p53 through post-translational modifications (PTMs) that guide p53 down pathways of cell cycle arrest and apoptosis.<sup>34,35</sup> Thus, in

addition to their induction of DNA damage in cancer cells, there is a boost of cell killing due to activation of wild-type p53. This is one of theoretical benefits of combining a putative mutant p53 reactivator with cytotoxic chemotherapy or radiation, which is that there will be a boost of wild-type p53 activity to the effect of chemotherapy or radiation. We recently investigated this with ZMC1 and found that, surprisingly, cytotoxic chemotherapy and radiation are not more effective in combination.<sup>36</sup> We elucidated the mechanism for this and found that the ROS signal of ZMC1 induced the same PTMs on p53 that are typically performed by chemotherapy or radiation.<sup>36</sup> Since the ROS signal by ZMC1 is from the chelation of redox-active metals like Cu<sup>2+</sup>, we measured the affinity of ZMC1 for copper (K<sub>Cu</sub>) and determined it to be 10<sup>-17</sup> M. This is 10<sup>8</sup>-fold higher than its affinity for Zn<sup>2+</sup><sup>36</sup> and 10<sup>2</sup>-fold higher than high-affinity intracellular copper-binding proteins.<sup>37</sup> We hypothesized that if we could identify a zinc-binding scaffold that bound copper more weakly (and therefore generated less ROS) but at the same time kept its affinity for zinc in the same range, the molecule could induce a wild-type p53 conformation without generating an ROS signal that would induce PTMs on p53. We reasoned that such a zinc scaffold when combined with chemotherapy or radiation would be synergistic. As a proof of concept, we tested nitrilotriacetic acid (NTA) whose K<sub>Zn</sub> (17 nM) was in the same range as that of ZMC1.<sup>36</sup> NTA has poor pharmacological properties including poor cell membrane permeability due to its anionic character. To overcome this, we synthesized analogues that replaced the ionizable acids in NTA with nonionizable esters (NTA-MEE and NTA-DEE) that were more permeable (Figure 7). While the NTA compounds bound Zn<sup>2+</sup> with affinities similar to that of ZMC1, they also

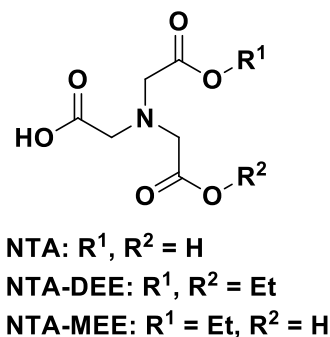
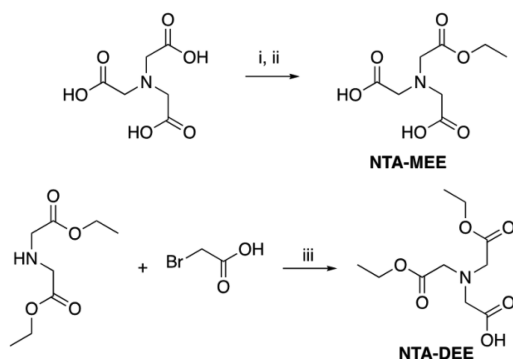


Figure 7. Structures of nitriloacetate derivatives.

bound copper much more weakly ( $10^6$ – $10^7$ -fold less than **ZMC1**). We found that the  $\text{Cu}^{2+}/\text{Zn}^{2+}$  selectivity ratio is much higher for **ZMC1** ( $10^8$ ) than for **NTA** and its esters ( $10$ – $10^3$ ).<sup>36</sup> At this ratio, the approximately  $10^5$ -fold greater availability of Zn in serum would be expected to largely preclude the formation of  $\text{Cu}^{2+}$  complexes in the blood.<sup>17</sup> We found that, indeed, these **NTA** esters could function as zinc metallochaperones to refold mutant p53, and they did produce less of an ROS signal. This decreased ROS signal lead to less cell killing due to a lack of induction of p53 PTMs. When combined with cytotoxic chemotherapy and radiation, however, we observed synergy in cell killing. Thus, we concluded that these zinc scaffolds, with a lower affinity for copper and a  $\text{Cu}^{2+}/\text{Zn}^{2+}$  selectivity in the range of  $10$ – $10^3$ , would represent a new class of ZMCs that would function as cytotoxic chemotherapy and radiation sensitizers in cancer cells with zinc-deficient mutant p53.

**Synthesis of the Nitriloacetates.** The nitrilotriacetate derivatives, **NTA-MEE** and **NTA-DEE**, were prepared via selective esterification or via alkylation, as shown in Scheme 10.

**Scheme 10.** (i)  $\text{Ac}_2\text{O}$ , Pyridine, and DMF; (ii) EtOH; and (iii) Dioxane



**C85 Combination Therapy.** In an effort to identify a zinc scaffold with better drug-like properties that could function as this new type of ZMC, we turned to the C-series. We selected a compound **C85** that had similar properties to **C69** but with the addition of the difluoromethylene (Figure 8A). We found from our SAR analysis that **C85** could induce a wild-type conformational change in the mutant p53 protein (Figure 8B); however, TOV-112D cells were less sensitive to **C85** than **ZMC1** ( $\text{EC}_{50}$  of **C85** as 151 nM vs **ZMC1** as 5 nM, 31-fold less than **ZMC1**). Likewise using the CellROX Green fluorescent agent in p53 null cells, we found that **C85** did in fact induce a smaller ROS signal in comparison to **ZMC1** (77% relative to **ZMC1**) or **C1** (170% relative to **ZMC1**). We measured the  $K_{\text{Cu}}$  of **C85** to be  $10^{-15}$  M and determined the  $\text{Cu}^{2+}/\text{Zn}^{2+}$  selectivity ratio to be  $10^7$ , one order of magnitude less than **ZMC1** (Figure 9). Although this reduction in selectivity does not meet the threshold for complete elimination of copper binding ( $10^5$ ), the  $\text{Cu}^{2+}$  affinity of this improved drug for copper no longer exceeds that of intracellular  $\text{Cu}^{2+}$ -binding proteins. Next, we performed combinatorial experiments with **C85** and  $\gamma$ -irradiation or etoposide in TOV-112D cells. We first subjected TOV-112D cells to **C85** and 5 Gy of radiation for 72 h and observed synergy. The  $\text{EC}_{50}$  decreased from 0.71  $\mu\text{M}$  (**C85** only) to 0.18  $\mu\text{M}$  (**C85** + 5 Gy of irradiation), 4-fold more effective in cell

growth inhibition (Figure 8C). Next, we combined the treatment of **C85** and etoposide. The  $\text{EC}_{50}$  decreased from 0.57  $\mu\text{M}$  (**C85** only) to 0.12  $\mu\text{M}$  (**C85** + etoposide), 4-fold more effective in cell growth inhibition (Figure 8D). These data indicate that **C85**, with its diminished  $\text{Cu}^{2+}/\text{Zn}^{2+}$  binding ratio, can function as a new type of ZMC that functions as a chemotherapy or radiation sensitizer in cancer cells with zinc-deficient mutant p53.

**ZMC1 and C85 Hydrolytic Stability Studies.** Many hydrazines are known to be toxic.<sup>38</sup> They are found in toxic mushrooms and even in some common button mushrooms.<sup>39</sup> Not all hydrazines are toxic, and many are approved drugs like carbidopa for Parkinson's disease, isoniazid against malaria, and phenelzine sulfate for depression. Nevertheless, the hydrolytic stability of our hydrazones is still a safety concern. We conducted stability studies with **ZMC1** and **C85** as representatives of the A-series and C-series in simulated gastric fluids (SGF, pH 1–2) and in phosphate-buffered saline (PBS, pH 7.4) at room temperature and at 37 °C when the compounds were found to be stable at room temperature ( $\sim 23$  °C (Supporting Information)). We used HPLC analysis at 220 and 254 nm and confirmed the peak identity by LC–MS. We found that **ZMC1** was not stable in SGF at room temperature, reaching an equilibrium with  $\sim 22\%$  of **ZMC1** remaining after 7 h. **C85** was much more stable, with  $>92$  and  $>82\%$  remaining after 6 h in SGF at room temperature and 37 °C, respectively. To avoid the acidic environment of the gut, iv administration for therapeutic dosing of our compounds is under consideration. Stability in PBS is used as a rough model for plasma stability. The greater hydrolytic stability of **C85** in SGF demonstrates an additional advantage of the C-series over the A-series for potential development. Metabolic stability of our compounds has not yet been fully established, but Pelivan *et al.* evaluated the metabolic stability of **A1** (their compound **9**) by incubation for 2 h with cell-free human liver microsomes followed by analysis with HPLC–HRMS and did not report observing hydrazine or ketone released from the reactions.<sup>24</sup> Many metabolites were observed, but the release of hydrazine was not among them.

## CONCLUSIONS

Due to the high frequency of missense p53 mutations in many types of cancers, the discovery and development of mutant p53 reactivators remains a large unmet need. Zinc metallochaperones represent a novel and viable strategy to meet this need; while thiosemicarbazones may still be a viable path forward, there remains a need to continue to identify alternative zinc scaffolds that can function as ZMCs. As the mechanism of action of ZMCs is novel, here, we provide evidence that the benzothiazolyl, benzoxazolyl, and benzimidazolyl hydrazones do in fact function as zinc metallochaperones both *in vitro* and *in vivo*.

As with any drug development program, establishing assays for SAR is paramount for successful identification of a clinical candidate. However, due to the uniqueness and complexity of the ZMC mechanism, the strategy of which assays would be best suited for this was not immediately obvious. We think that at minimum, the measurements of the  $K_{\text{Zn}}$  and the  $\text{EC}_{50}$  in a p53<sup>R175H</sup> tumor cell line (and perhaps a p53 null cell line to demonstrate specificity), along with the conformational antibody assay, are most important initially for SAR development. We determined that the upper limit of range in  $K_{\text{Zn}}$  for a scaffold to function as a ZMC is approximately 200 nM, which

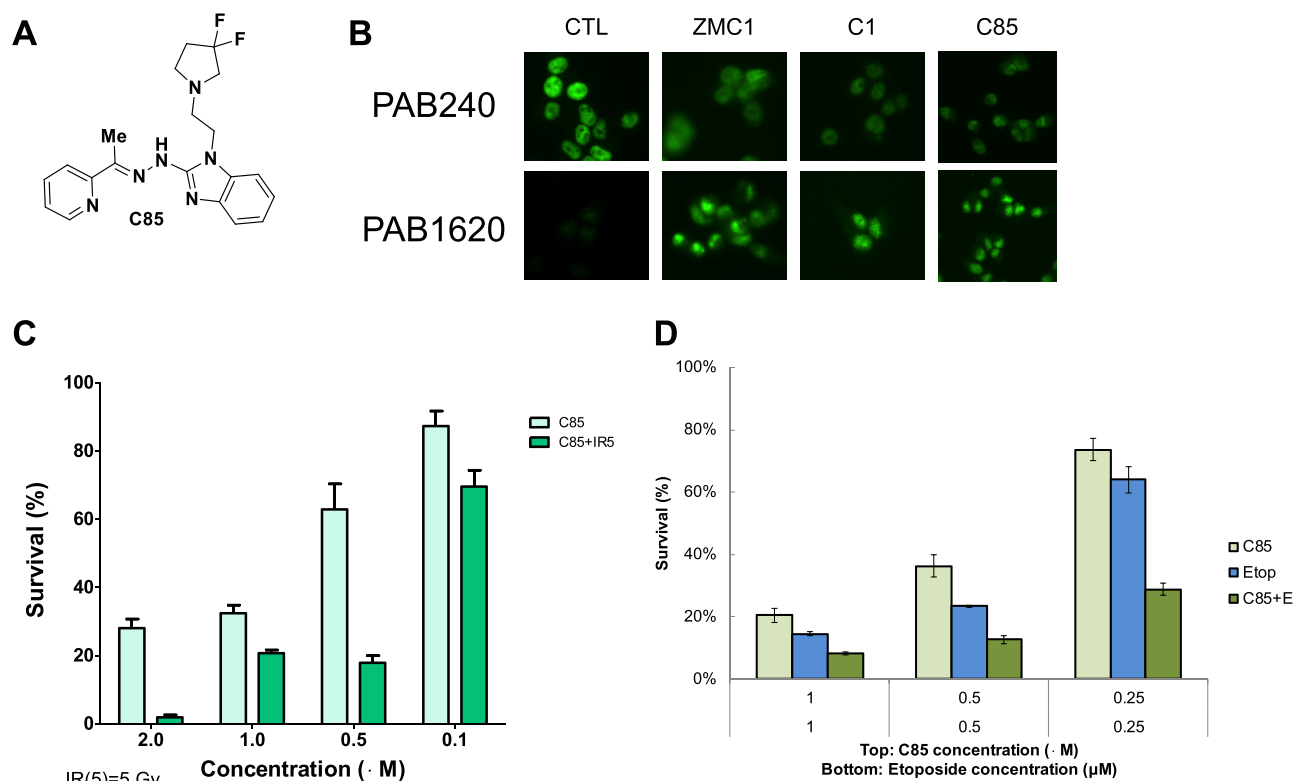


Figure 8. Combinatorial therapy of C85 and irradiation and chemotherapy drug.

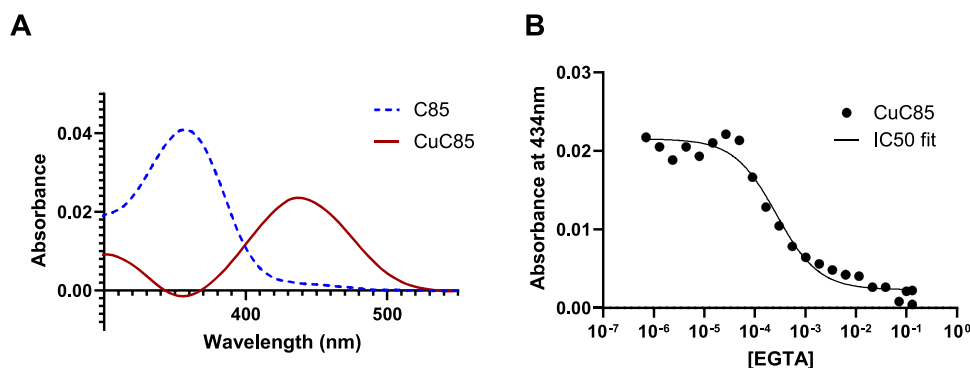


Figure 9. Copper affinity of C85.

is very helpful. We cannot, at this time, determine the lower limit of this range with high accuracy as none of the modifications we designed in the SAR around **ZMC1** increased its affinity for zinc significantly. In addition, we have not identify other metal ion chelator scaffolds that bound zinc more tightly than **ZMC1**, with the exception of EDTA. EDTA is one in which we have found that zinc binds so tightly that it will not donate zinc to p53; however, its  $K_{Zn}$  is  $10^{-16}$  M (as opposed to  $10^{-8}$  M for **ZMC1**).

Thiosemicarbazones are relatively easy to prepare, but the molecules can exist in many interchangeable stereoisomers, conformers, and metal complexes, which sometimes makes their chemical analysis and biological effects difficult to deconvolute. Very few drugs (4 hits in DrugBank) incorporating a thiosemicarbazone functional group have made it to the market and stayed on the market.<sup>40</sup> Their interactions with metals ions are numerous, and differences between complexes can be subtle. We explored using (pyridinyl)ethylidene-hydrazineyl)benzothiazole, benzoxazole, benzimidazole, and

imidazole compounds as possible zinc-binding and p53 refolding agents. Although we have not yet exhausted all the possible optimized analogues around these fragments, we did not identify analogues that were better than **ZMC1**. Initially, the benzothiazole C-series appeared to be the most promising, but its low solubility led us to add solubilizing groups that introduced liabilities in the hERG channel and other receptors. **ZMC1** and other highly active analogues are more hydrophilic than the benzothiazoles, benzimidazoles, and to a lower extent to the benzoxazoles. In future work, more efforts would be put into development of the benzoxazole series in addition to exploring more carefully the type and spacing of solubilizing groups.<sup>41</sup> Bioisosteres of the thiosemicarbazones will also be explored.

In theory, improving the ionophore activity to increase intracellular zinc will drive potency. We previously demonstrated this by synthesizing a neutral 2:1 complex of **ZMC1** to  $Zn^{2+}$  ( $Zn(ZMC1)_2$ ) and found enhancement in potency as compared to **ZMC1** alone, both *in vitro* and *in vivo*.<sup>10</sup> However



it is important to understand that with this mechanism, there are other cellular factors that can contribute to potency, such as expression of zinc homeostatic genes that regulate intracellular zinc levels. Zinc homeostatic mechanisms are dysregulated in certain cancers and particularly in breast cancer where zinc levels are higher in cancerous cells compared to normal mammary epithelial cells. In addition, the expression of zinc homeostatic genes is different across breast cancer subtypes (luminal, basal, and triple-negative breast cancer).<sup>42</sup> Thus, it is possible that variations in expression of these genes among tumors may cause variation in response to ZMCs.

The finding that **C1** is less toxic than **ZMC1** in acute *in vivo* toxicity assays is a validation of the general design principle that replacing the thiocarbamoyl moiety of a TSC with a benzothiazolyl, benzoxazolyl, or benzimidazolyl moiety reduces toxicity (as well as producing an increase in hydrolytic stability). The high degree of binding of many of the C-series analogues to 5HT receptors, opiate  $\mu$  receptors, hERG, and ion channels is a complication that may be addressed by careful modifications to the scaffold.

The finding that **C85** exhibits the type of reduced  $\text{Cu}^{2+}$  affinity and  $\text{Cu}^{2+}/\text{Zn}^{2+}$  selectivity ratio that would allow it to function as a chemotherapy and radiation sensitizer is a significant finding in this study. Up to now, the compounds we have identified that could provide this proof of concept were not suitable pharmacological agents. Using the 3,3'-difluoromethylpiperazine group of **C85** was an attempt to reduce the basicity of nitrogen, thereby reducing the risks of interacting with hERG and other receptors. Unfortunately, the CEREP screen revealed that this change was not sufficient to avoid these issues. While we still need to conduct screens for alternative zinc-binding scaffolds with diminished copper selectivity, we can conclude that simply preventing the compound from competing for intracellular copper produces powerful synergy. This new class of ZMC that functions as chemotherapy and radiation sensitizers would presumably lead to compounds that would be better tolerated. Moreover, because cytotoxic chemotherapy and radiation still remain the most common therapeutic modalities in oncology today, such a ZMC would potentially have a significant impact in oncology.

## ■ EXPERIMENTAL SECTION

**Cell Lines and Chemicals.** TOV-112D (p53<sup>R175H</sup>) and MDA-MB-468 (p53<sup>R273H</sup>) were purchased from ATCC and cultured in the DMEM with 10% FBS. Cell lines were authenticated by examination of morphology and growth characteristics. All chemicals were purchased from Sigma-Aldrich or otherwise indicated.

**Synthesis of the Compounds. General Information.** The reagents were purchased and used without additional purifications. LC–MS was performed on a Shimadzu system: LC–MS 2010A using a 10  $\mu\text{L}$  injection on a SunFire C18 column (3.5  $\mu\text{m}$ , 4.6  $\times$  50 mm) at a temperature of 40 °C with a 4 min gradient from 5% A to 100% B (solvent A: 0.1% TFA in water and solvent B: 0.1% TFA in acetonitrile) at a flow rate of 2 mL/min. The detection used dual channel UV at 220 and 254 nm (mass detection CDL voltage: –10 V). Alternatively, LC–MS was performed on an Agilent 1100 system with a Waters Micromass ZQ spectrometer using a 5  $\mu\text{L}$  injection on an XBridge C18 (3.5  $\mu\text{m}$ , 4.6  $\times$  50 mm) column at a temperature of 40 °C with a 3 min gradient from 5% A to 95% B (solvent A: 10 mM ammonium formate in water and solvent B: acetonitrile) at a flow rate of 2 mL/min. The detection used a diode array scanning from 190 to 600 nm or with dual wavelength detectors at 220 and 254 nm (mass detection cone voltage: 30 V). NMR was obtained on a Varian VNMR5 500 MHz or Bruker NMR 400 MHz in chloroform-*d* (<sup>1</sup>H:  $\delta$

7.26; <sup>13</sup>C:  $\delta$  77.00), DMSO-*d*<sub>6</sub> (<sup>1</sup>H:  $\delta$  2.50; <sup>13</sup>C:  $\delta$  39.52), or methanol-*d*<sub>4</sub> (<sup>1</sup>H:  $\delta$  3.31; <sup>13</sup>C:  $\delta$  49.00). The HRMS analyses were performed using a Bruker Apex 7T FTMS, using an ESI ion source in a positive mode (capillary exit voltage: 330 V).

Unless otherwise stated, the purities of the final compounds were equal to or greater than 95% by LC–MS analysis. The purities were confirmed with <sup>1</sup>H NMR to look for residual solvents or non-UV-active impurities. In addition, HRMS of most of the key compounds was obtained.

**Compounds Were Synthesized by the Rutgers Molecular Design and Synthesis Group.** **Methyl Hydrazinecarbodithioate (1).** To a solution of KOH (5.6 g, 100 mmol, 1 equiv) in water (10 mL) was added *i*-PrOH (10 mL). The solution was cooled to 0 °C followed by addition of hydrazine hydrate (79% solution in water) (6.15 mL, 100 mmol, 1 equiv). Carbon disulfide (6.0 mL, 100 mmol, 1 equiv) was added dropwise over 30 min, maintaining temperature below 10 °C, and the reaction was stirred for an additional hour at 0 °C. While remaining in an ice bath, methyl iodide (6.2 mL, 100 mmol, 1 equiv) was added over 30 min and the reaction was allowed to stir for an additional hour at 0 °C. The white solid precipitated from solution was filtered, washed with cold water, and dried under vacuum. The solid was washed through the filter and recrystallized in DCM to afford the title compound (**1**) (5.25 g, 43 mmol, 43% yield) as a white solid after filtration and drying under vacuum.

**Methyl (E)-2-(1-(Pyridin-2-yl)ethylidene)hydrazine-1-carbodithioate (2).** To a solution of methyl hydrazinecarbodithioate (**1**) (19.4 g, 160 mmol) in *i*-PrOH (50 mL) was added 1-(pyridin-2-yl)ethan-1-one (19.62 g, 162 mmol). After stirring for 2 h at 60 °C, the reaction was cooled to room temperature. The precipitated product was filtered and washed with *i*-PrOH. The solid was dried under vacuum to afford methyl (E)-2-(1-(pyridin-2-yl)ethylidene)hydrazine-1-carbodithioate (**2**) (37.2 g) as a light yellow solid. MS: 226.2 [M + H]<sup>+</sup>.

**(E)-N'-(1-(Pyridin-2-yl)ethylidene)azetidine-1-carbothiohydrazide (ZMC1).** Methyl (E)-2-(1-(pyridin-2-yl)ethylidene)hydrazine-1-carbodithioate (**2**) (19.7 g, 87.6 mmol) was dissolved in MeOH (400 mL) with heating. Azetidine (6 g, 105 mmol) was added dropwise over 15 min, and the reaction was stirred for 16 h at 60 °C. Overnight crystallization at 0 °C afforded (E)-N'-(1-(pyridin-2-yl)ethylidene)azetidine-1-carbothiohydrazide (**ZMC1**) (16.5 g, 70.5 mmol, 97.4% purity by HPLC) as a crystalline white solid after being filtered, washed with *i*-PrOH, and dried under vacuum. <sup>1</sup>H NMR (400 MHz, DMSO-*d*<sub>6</sub>):  $\delta$  2.26 (m, 2H), 2.36 (s, 3H), 4.12 (m, 2H), 4.59 (m, 2H), 7.39 (m, 1H), 7.83 (dt, *J* = 7.96, 1.76 Hz, 1H), 7.94 (d, *J* = 8.04 Hz, 1H), 8.60 (d, *J* = 4.00 Hz, 1H), 10.24 (s, 1H, NH). MS: 235.1 [M + H]<sup>+</sup>. HRMS (MALDI) (*m/z*): [2M + Na<sup>+</sup>] calcd for (C<sub>11</sub>H<sub>14</sub>N<sub>4</sub>S)<sub>2</sub> + Na<sup>+</sup>, 491.17710; found, 491.17710.

**(E)-N,N-Dimethyl-2-(1-(pyridin-2-yl)ethylidene)hydrazine-1-carbothioamide (A1).** To a solution of methyl (E)-2-(1-(pyridin-2-yl)ethylidene)hydrazine-1-carbodithioate (**2**) (378 mg, 1.68 mmol, 1 equiv) in EtOH (5 mL) was added dimethylamine (40% in water) (1 mL). The reaction was heated overnight at 40 °C. After cooling to room temperature, the precipitated solid was filtered, washed with EtOH, and dried under vacuum to afford (E)-N,N-dimethyl-2-(1-(pyridin-2-yl)ethylidene)hydrazine-1-carbothioamide (**A1**) (235 mg, 1.06 mmol, 99.6% purity by HPLC) as a yellow solid. <sup>1</sup>H NMR (500 MHz, DMSO-*d*<sub>6</sub>):  $\delta$  9.61 (s, 1H), 8.80–8.59 (m, 1H), 8.16–7.95 (m, 1H), 7.92–7.77 (m, 1H), 7.61–7.34 (m, 1H), 3.36–3.27 (m, 6H), 2.63–2.39 (m, 3H). MS: 223.1 [M + H]<sup>+</sup>. Note: peaks have complex splitting from multiple conformational isomers. HRMS (MALDI) (*m/z*): [2M + Na<sup>+</sup>] calcd for (C<sub>10</sub>H<sub>14</sub>N<sub>4</sub>S)<sub>2</sub> + Na<sup>+</sup>, 467.17720; found, 467.17710.

**N-(1-(Pyridin-2-yl)piperidin-4-yl)hydrazinecarbothioamide (3).** To a suspension of di(1H-imidazol-1-yl)methanethione (199 mg, 1.17 mmol, 1 equiv) and 1-(pyridin-2-yl)piperidin-4-amine (250 mg, 1.17 mmol, 1 equiv) in THF (3 mL) was added triethylamine (195  $\mu\text{L}$ , 1.4 mmol, 1.2 equiv). After stirring for 3 h at room temperature, a solution of hydrazine hydrate (79% solution in water) (284  $\mu\text{L}$ , 5.85 mmol, 5 equiv) in methanol (10 mL) was added and the reaction was allowed to stir overnight at room temperature. The reaction was



determined complete by TLC (50% EtOAc/Hex) and concentrated under reduced pressure. The residue was partitioned in EtOAc/H<sub>2</sub>O and extracted 4× with EtOAc. The combined organics were dried over Na<sub>2</sub>SO<sub>4</sub>, filtered, and concentrated. The product was recrystallized from EtOAc, filtered, and dried under vacuum to give *N*-(1-(pyridin-2-yl)piperidin-4-yl)hydrazinecarbothioamide (**3**) (189 mg, 0.75 mmol) as a light yellow solid.

*(E)*-2-(1-(Pyridin-2-yl)ethylidene)-*N*-(1-(pyridin-2-yl)piperidin-4-yl)hydrazine-1-carbothioamide (**A4**). To a solution of 1-(pyridin-2-yl)ethan-1-one (87 mg, 0.72 mmol, 1 equiv) and *N*-(1-(pyridin-2-yl)piperidin-4-yl)hydrazinecarbothioamide (**3**) in DCM (5 mL) was added AcOH (4 drops). The reaction was stirred overnight at room temperature and determined complete by TLC (10% MeOH/DCM). The crude reaction was partitioned in DCM and NaHCO<sub>3</sub>(sat, aq) and extracted 3× with DCM. The combined organics were dried over Na<sub>2</sub>SO<sub>4</sub>, filtered, and concentrated. The residue was purified by silica gel chromatography (EtOAc → 5% MeOH/DCM). Product containing fractions were concentrated and recrystallized from EtOAc to give a white solid, (*E*)-2-(1-(pyridin-2-yl)ethylidene)-*N*-(1-(pyridin-2-yl)piperidin-4-yl)hydrazine-1-carbothioamide (**A4**) (107 mg, 0.30 mmol, 99.3% purity by HPLC), which was filtered and dried under vacuum. <sup>1</sup>H NMR (400 MHz, CDCl<sub>3</sub>): δ 1.76 (ddd, *J* = 15.33, 11.72, 3.92 Hz, 2H), 2.30 (m, 2H), 2.42 (s, 3H), 3.04 (dt, *J* = 13.73, 2.40 Hz, 2H), 3.72 (m, 2H), 4.57 (m, 1H), 7.16 and 7.19 (E/Z d, 1.56 Hz, 1H), 7.21 and 7.24 (E/Z m, 1H), 7.30 (ddd, *J* = 5.87, 4.92, 1.04 Hz), 7.52 (br. d, *J* = 8.16 Hz, 1H, NH), 7.72 (dt, *J* = 7.76, 1.72 Hz, 1H), 7.90 (d, *J* = 8.04 Hz, 1H), 8.11 (dd, *J* = 4.44, 1.32 Hz, 1H), 8.35 (d, *J* = 2.68 Hz, 1H), 8.61 (d, *J* = 4.12 Hz, 1H), 8.68 (br. s, 1H, NH). MS: 287.0 [M + H]<sup>+</sup>.

*Methyl (Z)-N-((E)-1-(Pyridin-2-yl)ethylidene)azetidine-1-carbohydrazonothioate (A5)*. To a solution of (*E*)-*N'*-(1-(pyridin-2-yl)ethylidene)azetidine-1-carbothiohydrazide (**ZMC1**) (248 mg, 1 mmol, 1 equiv) in EtOH (4 mL) and DCM (4 mL) was added MeI (68.5 μL, 1.1 mmol, 1.1 equiv). After stirring for 2 h at room temperature, the reaction was determined complete by TLC (5% MeOH/DCM) and concentrated under reduced pressure. The product was recrystallized from EtOH, sonicated, and filtered. The solid was dried under high vacuum to afford the title compound methyl (*Z*)-*N*-((*E*)-1-(pyridin-2-yl)ethylidene)azetidine-1-carbohydrazonothioate (**A5**) (237.2 mg, 0.96 mmol, 100% purity by HPLC) as a light orange solid. <sup>1</sup>H NMR (400 MHz, DMSO-*d*<sub>6</sub>): δ 8.55 (ddd, *J* = 4.9, 1.8, 0.9 Hz, 1H), 7.99 (m, 1H), 7.76 (q, *J* = 8.1 Hz, 1H), 7.32 (q, *J* = 7.0, 6.6 Hz, 1H), 4.26 (t, *J* = 7.6 Hz, 2H), 4.12 (t, *J* = 7.7 Hz, 2H), 2.39 (d, *J* = 2.4 Hz, 3H), 2.33 (s, 3H), 2.32–2.20 (m, 2H). MS: 248.95 [M + H]<sup>+</sup>.

*(E)*-2-(1-Hydrazineylideneethyl)pyridine (**4**). To a solution of 1-(pyridin-2-yl)ethan-1-one (2.0 g, 16.5 mmol, 1 equiv) in EtOH (5 mL) was added hydrazine hydrate (79% solution in water) (5 mL). The reaction was heated 4 h at 90 °C, determined complete by TLC, concentrated under reduced pressure, and dried overnight under high vacuum to afford (*E*)-2-(1-hydrazineylideneethyl)pyridine (**4**) (2.1 g, 15.5 mmol) as a white solid that was used without further purification.

*(E)-N'-(1-(Pyridin-2-yl)ethylidene)azetidine-1-carbohydrazide (A6)*. To a solution of (*E*)-2-(1-hydrazineylideneethyl)pyridine (**4**) (300 mg, 2.2 mmol, 1 equiv) in DCM (3 mL) at 0 °C was added a solution of 4-nitrophenyl carbonochloridate (447 mg, 2.2 mmol, 1 equiv) in DCM (3 mL) dropwise over 10 min. The reaction was warmed to room temperature and stirred for 90 min to give 4-nitrophenyl (*E*)-2-(1-(pyridin-2-yl)ethylidene)hydrazine-1-carboxylate (**5**). MS: 300.90 [M + H]<sup>+</sup>. The reaction was cooled to 0 °C followed by addition of triethylamine (930 μL, 6.7 mmol, 3 equiv) and azetidine (300 μL, 4.4 mmol, 1 equiv). The reaction was stirred overnight, slowly warming to room temperature. The reaction was determined complete by LC–MS and partitioned in DCM/H<sub>2</sub>O. The aqueous layer was extracted 2× with DCM, dried over Na<sub>2</sub>SO<sub>4</sub>, filtered, and concentrated. The residue was purified by silica gel chromatography (1% → 2% → 5% MeOH/DCM). Product fractions were concentrated followed by recrystallization in EtOAc. The solid was filtered, washed with EtOAc, and dried under vacuum to give (*E*)-*N'*-(1-(pyridin-2-yl)ethylidene)azetidine-1-carbohydrazide (**A6**) (103

mg, 0.47 mmol, 99.0% purity by HPLC) as a white solid. <sup>1</sup>H NMR (400 MHz, CDCl<sub>3</sub>): δ 2.28 (s, 3H), 2.32 (t, *J* = 7.68 Hz, 1H), 2.36 (t, *J* = 7.80 Hz, 1H), 4.35 (t, *J* = 7.36 Hz, 4H), 7.24 (ddd, *J* = 3.52, 2.48, 1.08 Hz, 1H), 7.66 (dt, *J* = 7.84, 1.76 Hz, 1H), 7.81 (s, 1H, NH), 7.91 (d, *J* = 8.08 Hz, 1H), 8.57 (d, *J* = 4.20 Hz, 1H). MS: 219 [M + H]<sup>+</sup>.

*Azetidine-1-carbothiohydrazide (6)*. To a mixture of di(1*H*-imidazol-1-yl)methanethione (4.38 g, 24.6 mmol, 1.15 equiv) and azetidine HCl (2.0 g, 21.4 mmol, 1 equiv) in THF (20 mL) was added triethylamine (4.47 mL, 32.1 mmol, 1.5 equiv). The reaction was stirred for 5 days at room temperature followed by removal of THF under reduced pressure to give a crude mixture of azetidin-1-yl(1*H*-imidazol-1-yl)methanethione. This mixture was taken up in EtOH (20 mL) followed by addition of hydrazine hydrate (2 mL). The reaction was heated at reflux for 3 h, cooled to room temperature, and concentrated under reduced pressure. The residue was partitioned in DCM/H<sub>2</sub>O, and the DCM layer was washed 2× with water, dried over Na<sub>2</sub>SO<sub>4</sub>, filtered, and evaporated to give azetidine-1-carbothiohydrazide (**6**) (917 mg, 7 mmol, 32% yield) as a white solid that was used without further purification.

*(E)-N'-(1-Phenylethylidene)azetidine-1-carbothiohydrazide (A9)*. To a solution of azetidine-1-carbothiohydrazide (**6**) (163 mg, 1.24 mmol, 1 equiv) and acetophenone (223 mg, 1.86 mmol, 1.5 equiv) in DCM (4 mL) was added AcOH (4 drops). After stirring overnight at room temperature, the reaction was determined complete by TLC (50% EtOAc/Hex) and concentrated under reduced pressure. Recrystallization from MeOH yielded the title compound (*E*)-*N'*-(1-phenylethylidene)azetidine-1-carbothiohydrazide (**A9**) (176 mg, 0.76 mmol) as a white solid. <sup>1</sup>H NMR (400 MHz, CDCl<sub>3</sub>): δ 2.33 (t, *J* = 7.80 Hz, 1H), 2.37 (t, *J* = 7.88 Hz, 1H), 4.33 (m, 2H), 4.69 (m, 2H), 7.37 (m, 3H), 7.65 (m, 2H), 8.63 (br. s, 1H, NH). MS: 234.1 [M + H]<sup>+</sup>.

*(E)-N'-(1-(Pyrazin-2-yl)ethylidene)azetidine-1-carbothiohydrazide (A10)*. To a solution of azetidine-1-carbothiohydrazide (**6**) (156 mg, 1.19 mmol, 1.0 equiv) and 1-(pyrazin-2-yl)ethan-1-one (152 mg, 1.25 mmol, 1.05 equiv) in DCM (6 mL) was added AcOH (4 drops). After stirring overnight at room temperature, the reaction was concentrated under reduced pressure and recrystallized from MeOH to afford (*E*)-*N'*-(1-(pyrazin-2-yl)ethylidene)azetidine-1-carbothiohydrazide (**A10**) (132 mg, 0.56 mmol, 99.2% purity by HPLC) as a crystalline white solid. <sup>1</sup>H NMR (400 MHz, CDCl<sub>3</sub>): δ 2.38 (t, *J* = 7.72 Hz, 1H), 2.42 (t, *J* = 7.88 Hz, 1H), 4.36 (br. t, *J* = 7.52 Hz, 1H), 4.73 (br. t, *J* = 7.40 Hz, 1H), 8.50 (d, *J* = 2.56 Hz, 1H), 8.53 (m, 1H), 8.78 (s, 1H, NH), 9.13 (m, 1H). MS: 236.1 [M + H]<sup>+</sup>.

*(E)-N'-(1-(6-Methylpyridin-2-yl)ethylidene)azetidine-1-carbothiohydrazide (A11)*. To a solution of azetidine-1-carbothiohydrazide (**6**) (102 mg, 0.78 mmol, 1 equiv) and 1-(6-methylpyridin-2-yl)ethan-1-one (126 mg, 0.93 mmol, 1.2 equiv) in DCM (5 mL) was added AcOH (4 drops). After stirring overnight at room temperature, the reaction was determined complete by TLC (50% EtOAc/Hex) and concentrated under reduced pressure. The resultant solid was recrystallized from MeOH, filtered, and dried under vacuum to give the title compound (*E*)-*N'*-(1-(6-methylpyridin-2-yl)ethylidene)-azetidine-1-carbothiohydrazide (**A11**) (30 mg, 0.12 mmol, 100% purity) as a white solid. <sup>1</sup>H NMR (400 MHz, CDCl<sub>3</sub>): δ 2.35 (m, 5H), 2.56 and 2.67 (E/Z s, 3H), 4.34 (m, 2H), 4.70 (m, 2H), 7.11 and 7.18 (E/Z d, *J* = 7.52 Hz, 1H), 7.30 and 7.65 (E/Z d, *J* = 8.00 Hz, 1H), 7.56 and 7.73 (E/Z t, *J* = 7.84 Hz, 1H), 8.71 (s, 1H, NH). MS: 248.9 [M + H]<sup>+</sup>.

*(E)-N'-(1-(3-Methylpyridin-2-yl)ethylidene)azetidine-1-carbothiohydrazide (A12)*. To a solution of azetidine-1-carbothiohydrazide (**6**) (100 mg, 0.77 mmol, 1 equiv) and 1-(6-methylpyridin-2-yl)ethan-1-one (123 mg, 0.91 mmol, 1.2 equiv) in DCM (5 mL) was added AcOH (4 drops). After stirring overnight at room temperature, the reaction was determined complete by TLC (50% EtOAc/Hex) and concentrated under reduced pressure. The resultant solid was recrystallized from MeOH, filtered, and dried under vacuum to give the title compound (*E*)-*N'*-(1-(3-methylpyridin-2-yl)ethylidene)-azetidine-1-carbothiohydrazide (**A12**) (23 mg, 0.093 mmol, 99.0% purity by HPLC) as a white solid after recrystallization from MeOH. Note: a significant amount of product was washed into the filtrate. <sup>1</sup>H

NMR (400 MHz,  $\text{CDCl}_3$ ):  $\delta$  2.27 (m, 6H), 2.43 (m, 2H), 4.37 (m, 4H), 7.19 and 7.26 (E/Z dd,  $J = 7.72, 4.72$  Hz, 1H), 7.56 and 7.61 (E/Z d,  $J = 7.68$  Hz, 1H), 8.40 and 8.66 (E/Z br. s, 1H, NH), 8.46 and 8.55 (E/Z d,  $J = 3.76$  Hz, 1H). MS: 248.9  $[\text{M} + \text{H}]^+$ .

(*E*)-*N'*-(2,2-Dimethyl-1-(pyridin-2-yl)propylidene)azetidine-1-carbothiohydrazide (**A13**). To a solution of azetidine-1-carbothiohydrazide (**6**) (116 mg, 0.88 mmol, 1 equiv) and 2,2-dimethyl-1-(pyridin-2-yl)propan-1-one (123 mg, 0.91 mmol, 1.2 equiv) in DCM (5 mL) was added AcOH (4 drops). After stirring overnight at room temperature, the reaction was determined complete by TLC (50% EtOAc/Hex) and concentrated under reduced pressure. The crude residue was purified by silica gel chromatography (20%  $\rightarrow$  30% EtOAc/Hex), and the concentrated product fractions were recrystallized from EtOAc/Hex. The crystallized solid was filtered and dried under high vacuum to afford (*E*)-*N'*-(2,2-dimethyl-1-(pyridin-2-yl)propylidene)azetidine-1-carbothiohydrazide (**A13**) (9.3 mg, 0.034 mmol, 99.0% purity by HPLC).  $^1\text{H}$  NMR (400 MHz,  $\text{CDCl}_3$ ):  $\delta$  1.18 (s, 9H), 2.29 (t,  $J = 7.76$  Hz, 1H), 2.33 (t,  $J = 7.84$  Hz, 1H), 4.26 (t,  $J = 7.36$  Hz, 1H), 4.66 (t,  $J = 7.72$  Hz, 1H), 7.18 (d,  $J = 7.76$  Hz, 1H), 7.35 (ddd,  $J = 6.00, 4.92, 1.12$  Hz, 1H), 7.81 (dt,  $J = 7.76, 1.76$  Hz, 1H), 8.26 (br. s, 1H, NH), 8.76 (d,  $J = 4.80$  Hz, 1H). MS: 277.1  $[\text{M} + \text{H}]^+$ .

1-(4-(Dimethylamino)pyridin-2-yl)ethan-1-one (**7**). 1-(4-Chloropyridin-2-yl)ethan-1-one (500 mg, 3.2 mmol, 1 equiv) was taken up in dimethylamine (40% in water) (3.5 mL) and heated overnight at 100  $^\circ\text{C}$  in a sealed reaction vial. The reaction was determined complete by TLC (50% EtOAc/Hex) and concentrated under reduced pressure. Silica gel chromatography (50% EtOAc/Hex  $\rightarrow$  EtOAc) afforded 1-(4-(dimethylamino)pyridin-2-yl)ethan-1-one (**7**) (357 mg, 2.2 mmol) as a light yellow oil after concentration of product fractions.

(*E*)-*N'*-(1-(4-(Dimethylamino)pyridin-2-yl)ethylidene)azetidine-1-carbothiohydrazide (**A14**). To a solution of azetidine-1-carbothiohydrazide (**6**) (139 mg, 1.06 mmol, 1.1 equiv) and 1-(4-(dimethylamino)pyridin-2-yl)ethan-1-one (**7**) (150 mg, 0.96 mmol, 1 equiv) in DCM (4 mL) was added AcOH (4 drops). After stirring overnight, the reaction was determined complete by TLC (10% MeOH/DCM) and concentrated under reduced pressure. Purification by silica gel chromatography (5%  $\rightarrow$  10% MeOH/DCM) followed by recrystallization from MeOH yielded the title compound (*E*)-*N'*-(1-(4-(dimethylamino)pyridin-2-yl)ethylidene)azetidine-1-carbothiohydrazide (**A14**) (27.4 mg, 0.1 mmol, 100% purity by HPLC) as a white solid.  $^1\text{H}$  NMR (400 MHz,  $\text{CDCl}_3$ ):  $\delta$  2.34 (m, 5H), 3.02 (s, 6H), 4.34 (m, 2H), 4.70 (m, 2H), 6.49 and 6.54 (E/Z dd,  $J = 6.04, 2.64$  Hz, 1H), 6.62 and 7.08 (E/Z d,  $J = 2.44$  Hz, 1H), 8.26 (m, 1H), 8.71 (br. s, 1H, NH). MS: 278.0  $[\text{M} + \text{H}]^+$ .

(*E*)-2-(2-(1-(Pyridin-2-yl)ethylidene)hydrazinyl)benzo[d]thiazole (**C1**). 1-(Pyridin-2-yl)ethan-1-one (204  $\mu\text{L}$ , 1.82 mmol, 1 equiv) and 2-hydrazinylbenzo[d]thiazole (300 mg, 1.82 mmol, 1 equiv) were dissolved in EtOH (10 mL) followed by addition of AcOH (10 drops). The reaction was stirred overnight at room temperature and determined complete by TLC (50% EtOAc/Hex). The crude reaction was concentrated under reduced pressure, recrystallized from MeOH, sonicated, and filtered to give the title compound (*E*)-2-(2-(1-(pyridin-2-yl)ethylidene)hydrazinyl)benzo[d]thiazole (**C1**) (324 mg, 1.21 mmol, 100% purity by HPLC) as a white solid after drying under high vacuum.  $^1\text{H}$  NMR (400 MHz,  $\text{CDCl}_3$ ):  $\delta$  2.44 (s, 3H), 7.19 (dt,  $J = 7.2, 1.01$  Hz, 1H), 7.26 (m, 1H), 7.36 (dt,  $J = 7.2, 1.01$  Hz, 1H), 7.62 (d,  $J = 7.96$  Hz, 1H), 7.71 (d,  $J = 7.08$  Hz, 1H), 7.74 (dt,  $J = 7.76, 1.76$  Hz, 1H), 8.18 (d,  $J = 8.12$  Hz, 1H), 8.60 (br. d,  $J = 4.32$  Hz, 1H), 9.14 (br. s, 1H, NH). MS: 269.0  $[\text{M} + \text{H}]^+$ . HRMS (MALDI) ( $m/z$ ):  $[\text{M} + \text{H}]^+$  calcd for  $\text{C}_{14}\text{H}_{12}\text{N}_4\text{S} + \text{H}^+$ , 269.08620; found, 269.08550.

(*E*)-2-(2-(1-(Pyridin-2-yl)ethylidene)hydrazinyl)benzo[d]oxazole (**C2**). 2-Hydrazinylbenzo[d]oxazole (1.33 g, 8.9 mmol, 1 equiv) and 1-(pyridin-2-yl)ethan-1-one (1.0 mL, 8.92 mmol, 1 equiv) were dissolved in EtOH (20 mL) followed by addition of AcOH (10 drops). After stirring overnight at room temperature, the reaction was determined complete by LC–MS and the precipitated solid was filtered. Recrystallization from MeOH yielded the title compound

(*E*)-2-(2-(1-(pyridin-2-yl)ethylidene)hydrazinyl)benzo[d]oxazole (**C2**) (1.81 g, 7.17 mmol, 100% purity by HPLC) as a white solid after drying the solid under high vacuum.  $^1\text{H}$  NMR (400 MHz,  $\text{CDCl}_3$ ):  $\delta$  2.48 (s, 3H), 7.16 (br. t,  $J = 7.28$  Hz, 1H), 7.28 (m, 2H), 7.44 (br. d,  $J = 7.28$  Hz, 1H), 7.51 (br. d,  $J = 7.04$  Hz), 7.73 (t,  $J = 7.40$  Hz, 1H), 8.27 (br. d,  $J = 7.28$  Hz, 1H), 8.60 (d,  $J = 4.72$  Hz, 1H), 8.85 (br. s, 1H, NH). MS: 253.1  $[\text{M} + \text{H}]^+$ . HRMS (MALDI) ( $m/z$ ):  $[\text{2M} + \text{H}^+]$  calcd for  $(\text{C}_{14}\text{H}_{12}\text{N}_4\text{O})_2 + \text{H}^+$ , 505.20930; found, 505.20950.

(*E*)-1-Methyl-2-(2-(1-(pyridin-2-yl)ethylidene)hydrazinyl)-1H-benzo[d]imidazole (**C9**). 2-Hydrazinyl-1-methyl-1H-benzo[d]imidazole (109 mg, 0.68 mmol, 1 equiv) and 1-(pyridin-2-yl)ethan-1-one (76  $\mu\text{L}$ , 0.68 mmol, 1 equiv) were dissolved in EtOH (5 mL) followed by addition of AcOH (4 drops). After stirring overnight at room temperature, the reaction was determined complete by LC–MS. Purification by silica gel chromatography (50% EtOAc/Hex  $\rightarrow$  EtOAc) followed by recrystallization from 5:1 Hex/EtOAc yielded the title compound (*E*)-1-methyl-2-(2-(1-(pyridin-2-yl)ethylidene)hydrazinyl)-1H-benzo[d]imidazole (**C9**) (110 mg, 0.41 mmol, 99% purity by HPLC) as a yellow solid after drying the solid under high vacuum.  $^1\text{H}$  NMR (400 MHz,  $\text{CDCl}_3$ ):  $\delta$  2.59 (s, 3H), 3.54 (s, 3H), 7.02 (m, 4H), 7.21 (br. t,  $J = 5.50$  Hz, 1H), 7.67 (t,  $J = 7.88$  Hz, 1H), 8.08 (d,  $J = 8.00$  Hz, 1H), 8.60 (d,  $J = 4.72$  Hz, 1H), 9.10 (br. s, 1H, NH). MS: 266.3  $[\text{M} + \text{H}]^+$ . HRMS (MALDI) ( $m/z$ ):  $[\text{2M} + \text{H}^+]$  calcd for  $(\text{C}_{15}\text{H}_{13}\text{N}_5)_2 + \text{H}^+$ , 531.27240; found, 531.27280.

(*E*)-2-(1-(2-(Benzo[d]thiazol-2-yl)hydrazineylidene)ethyl)-*N,N*-dimethylpyridin-4-amine (**C21**). 1-(4-(Dimethylamino)pyridin-2-yl)ethan-1-one (**7**) (103 mg, 0.63 mmol, 1 equiv) and 2-hydrazinylbenzo[d]thiazole (104 mg, 0.63 mmol, 1 equiv) were dissolved in EtOH (5 mL). After the addition of AcOH (4 drops), the reaction was stirred overnight at room temperature. The reaction was determined complete by LC–MS and was concentrated under reduced pressure. The residue was partitioned in EtOAc/ $\text{NaHCO}_3$ (sat, aq) and extracted 3 $\times$  with EtOAc. The combined organic was dried over  $\text{Na}_2\text{SO}_4$ , filtered, and concentrated. The residue was purified by silica gel chromatography (2%  $\rightarrow$  5%  $\rightarrow$  10% MeOH/DCM). The combined product containing fractions were concentrated under reduced pressure and recrystallized from EtOH. The crystalline solid was filtered and washed with EtOH, and the solid was dried under high vacuum to afford (*E*)-2-(1-(2-(benzo[d]thiazol-2-yl)hydrazineylidene)ethyl)-*N,N*-dimethylpyridin-4-amine (**C21**) (52.3 mg, 0.17 mmol, 96.9% purity by HPLC) as a pale red solid.  $^1\text{H}$  NMR (400 MHz, chloroform-*d*):  $\delta$  8.91 (s, 1H), 8.26 (dd,  $J = 19.8, 6.0$  Hz, 1H), 7.69 (t,  $J = 8.0$  Hz, 1H), 7.62 (d,  $J = 7.3$  Hz, 1H), 7.42 (s, 1H), 7.33 (dt,  $J = 17.4, 7.9$  Hz, 1H), 7.15 (dt,  $J = 24.7, 7.4$  Hz, 1H), 6.53 (t,  $J = 5.5$  Hz, 1H), 3.09 (d,  $J = 11.3$  Hz, 6H), 2.41 (s, 3H). MS: 312.1  $[\text{M} + \text{H}]^+$ .

(*E*)-2-(2-(1-(Pyridin-2-yl)ethylidene)hydrazineyl)quinoline (**C22**). 2-Hydrazineylquinoline (100 mg, 0.63 mmol, 1 equiv) and 1-(pyridin-2-yl)ethan-1-one (71  $\mu\text{L}$ , 0.63 mmol, 1 equiv) were dissolved in EtOH (5 mL) followed by addition of AcOH (4 drops). The reaction was determined complete by LC–MS, and the precipitated solid was filtered. Recrystallization of the resultant solid from MeOH gave the title compound (*E*)-2-(2-(1-(pyridin-2-yl)ethylidene)hydrazineyl)quinoline (**C22**) (65 mg, 0.25 mmol, 99.4% purity by HPLC) as a yellow/orange solid after drying the solid under high vacuum.  $^1\text{H}$  NMR (400 MHz, chloroform-*d*):  $\delta$  8.64–8.58 (m, 1H), 8.55 (s, 1H), 8.21 (d,  $J = 8.0$  Hz, 1H), 8.10 (d,  $J = 8.9$  Hz, 1H), 7.85–7.68 (m, 4H), 7.62 (ddd,  $J = 8.5, 7.1, 1.6$  Hz, 1H), 7.41–7.30 (m, 1H), 7.25–7.19 (m, 1H), 2.48 (s, 3H). MS: 262.9  $[\text{M} + \text{H}]^+$ .

6-(2-Methoxyethoxy)benzo[d]thiazol-2-amine (**8**). To a solution of 2-aminobenzo[d]thiazol-6-ol (500 mg, 3.0 mmol, 1 equiv) in DMF (30 mL) was added  $\text{Cs}_2\text{CO}_3$  (4.9 g, 15 mmol, 5 equiv) followed by 1-bromo-2-methoxyethane (310  $\mu\text{L}$ , 3.3 mmol, 1.1 equiv). The reaction was stirred overnight at room temperature and determined complete by TLC (10% MeOH/DCM). The crude reaction was partitioned in EtOAc/ $\text{H}_2\text{O}$ . After removal of the layer, the organic was further washed 2 $\times$  with  $\text{H}_2\text{O}$  and 1 $\times$  with brine. The organic was dried over  $\text{Na}_2\text{SO}_4$ , filtered, and concentrated. The residue was purified by silica gel chromatography (2%  $\rightarrow$  5% MeOH/DCM) followed by (25%  $\rightarrow$



50% EtOAc/Hex  $\rightarrow$  EtOAc). Product containing fractions were concentrated under reduced pressure and recrystallized from EtOAc. The solid was filtered and dried under high vacuum to afford 6-(2-methoxyethoxy)benzo[d]thiazol-2-amine (8) (251 mg, 1.1 mmol) as a white solid.

**2-Hydrazineyl-6-(2-methoxyethoxy)benzo[d]thiazole (9).** To a solution of 6-(2-methoxyethoxy)benzo[d]thiazol-2-amine (8) (150 mg, 0.67 mmol, 1 equiv) in ethylene glycol (3 mL) was added hydrazine hydrate (195  $\mu$ L, 4.0 mmol, 6 equiv) followed by concd HCl (37% aq) (195  $\mu$ L, 2.3 mmol, 3.5 equiv). The reaction was heated overnight at 110  $^{\circ}$ C. There was very little conversion to the desired product, so a mixture of hydrazine hydrate (400  $\mu$ L, 8.2 mmol, 12 equiv) and concd HCl (37% aq) (400  $\mu$ L, 4.6 mmol, 7 equiv) was added and the reaction was heated overnight at 140  $^{\circ}$ C in a sealed reaction vial. The reaction was determined complete by TLC (5% MeOH/DCM), and the reaction was partitioned in DCM/H<sub>2</sub>O and extracted 3 $\times$  with DCM. The combined organic was dried over Na<sub>2</sub>SO<sub>4</sub>, filtered, and concentrated. The residue was recrystallized from EtOAc to afford the title compound 2-hydrazineyl-6-(2-methoxyethoxy)benzo[d]thiazole (9) (77.7 mg, 0.32 mmol) as a light brown solid.

**(E)-6-(2-Methoxyethoxy)-2-(2-(1-(pyridin-2-yl)ethylidene)hydrazineyl)benzo[d]thiazole AcOH (C23).** 2-Hydrazineyl-6-(2-methoxyethoxy)benzo[d]thiazole (9) (60 mg, 0.25 mmol, 1 equiv) and 1-(pyridin-2-yl)ethan-1-one (28  $\mu$ L, 0.25 mmol, 1 equiv) were dissolved in EtOH (5 mL) followed by addition of AcOH (4 drops). The reaction was determined complete by LC–MS and concentrated under reduced pressure. The resultant solid was purified by silica gel chromatography (25%  $\rightarrow$  50% EtOAc/Hex  $\rightarrow$  EtOAc) followed by recrystallization of product fractions from EtOH to give the title compound (E)-6-(2-methoxyethoxy)-2-(2-(1-(pyridin-2-yl)ethylidene)hydrazineyl)benzo[d]thiazole AcOH (C23) (44.7 mg, 0.11 mmol, 99.3% purity by HPLC) as a white solid after drying the solid under high vacuum. <sup>1</sup>H NMR (acetate salt) (400 MHz, chloroform-*d*):  $\delta$  8.68–8.56 (m, 1H), 8.15 (d, *J* = 8.3 Hz, 1H), 7.72 (td, *J* = 7.7, 1.8 Hz, 1H), 7.45 (d, *J* = 8.8 Hz, 1H), 7.27–7.22 (m, 2H), 6.99 (dd, *J* = 8.8, 2.5 Hz, 1H), 4.26–4.11 (m, 2H), 3.88–3.71 (m, 2H), 3.47 (s, 3H), 2.48 (s, 3H), 2.14 (s, 3H). MS: 342.95 [M + H]<sup>+</sup>.

**2-(2-Chloro-1H-benzo[d]imidazol-1-yl)-N,N-dimethylethan-1-amine (10).** To a solution of 2-chloro-1H-benzo[d]imidazole (500 mg, 3.3 mmol, 1 equiv) in DMF (7 mL) at 0  $^{\circ}$ C was added NaH (60% dispersion) (394 mg, 9.8 mmol, 3 equiv). After stirring for 10 min, 2-chloro-N,N-dimethylethan-1-amine HCl (709 mg, 4.92 mmol, 1 equiv) was added and the reaction was allowed to stir overnight as it slowly warmed to room temperature. The reaction proceeded to roughly 60% completion by LC–MS but was quenched with water and partitioned in EtOAc/H<sub>2</sub>O. The organic was washed 2 $\times$  with water and 1 $\times$  with brine, dried over Na<sub>2</sub>SO<sub>4</sub>, filtered, and concentrated. The residue was purified by silica gel chromatography (EtOAc  $\rightarrow$  5% MeOH/DCM), and product containing fractions were concentrated to give 2-(2-chloro-1H-benzo[d]imidazol-1-yl)-N,N-dimethylethan-1-amine (10) (300 mg, 70% purity by LC–MS), which was used without further purification in the subsequent reaction. MS: 223.85 [M + H]<sup>+</sup>.

**2-(2-Hydrazineyl-1H-benzo[d]imidazol-1-yl)-N,N-dimethylethan-1-amine (11).** A mixture of 2-(2-chloro-1H-benzo[d]imidazol-1-yl)-N,N-dimethylethan-1-amine (10) (300 mg, 70% purity by LC–MS) in *i*-PrOH (2 mL) and hydrazine hydrate (2 mL) was heated overnight at 140  $^{\circ}$ C in a sealed reaction vial. The reaction was determined complete by LC–MS and concentrated under reduced pressure. The crude product was redissolved in *i*-PrOH and reconcentrated repeatedly until there was confidence that a majority of the excess hydrazine hydrate was removed. The title compound 2-(2-hydrazineyl-1H-benzo[d]imidazol-1-yl)-N,N-dimethylethan-1-amine (11) was used as is in the next reaction, assuming quantitative yield. MS: 219.90 [M + H]<sup>+</sup>.

**(E)-N,N-Dimethyl-2-(2-(2-(1-(pyridin-2-yl)ethylidene)hydrazineyl)-1H-benzo[d]imidazol-1-yl)ethan-1-amine HCl (C27).** To a solution of 2-(2-hydrazineyl-1H-benzo[d]imidazol-1-yl)-N,N-

dimethylethan-1-amine (11) (crude from the previous reaction) in EtOH (10 mL) was added 1-(pyridin-2-yl)ethan-1-one (300  $\mu$ L, excess) followed by AcOH (10 drops). The reaction was stirred overnight at room temperature and was determined complete by LC–MS. The crude reaction was partitioned in DCM/NaHCO<sub>3</sub>(sat, aq), and the aqueous was extracted 3 $\times$  with DCM. The combined organic was dried over Na<sub>2</sub>SO<sub>4</sub>, filtered, and concentrated. The residue was purified by basic alumina chromatography (50% EtOAc/Hex  $\rightarrow$  EtOAc), and product fractions were concentrated and repurified by silica gel chromatography (2%  $\rightarrow$  5%  $\rightarrow$  10% MeOH/DCM) to give the title compound (E)-N,N-dimethyl-2-(2-(2-(1-(pyridin-2-yl)ethylidene)hydrazineyl)-1H-benzo[d]imidazol-1-yl)ethan-1-amine (C27) (56.6 mg, free base) as a red/orange oil. This oil was dissolved in MeOH (3 mL), acidified with HCl (2 M in Et<sub>2</sub>O) (1 mL), and concentrated under reduced pressure. The concentrate was recrystallized from MeOH/Et<sub>2</sub>O, filtered, and dried under vacuum to give (E)-N,N-dimethyl-2-(2-(2-(1-(pyridin-2-yl)ethylidene)hydrazineyl)-1H-benzo[d]imidazol-1-yl)ethan-1-amine HCl (C27) (52 mg, 0.13 mmol, 100% purity by HPLC) as an orange solid. <sup>1</sup>H NMR (HCl salt) (500 MHz, DMSO-*d*<sub>6</sub>):  $\delta$  13.24 (s, 1H), 10.28 (s, 1H), 8.78 (dd, *J* = 6.0, 1.6 Hz, 1H), 8.52 (t, *J* = 7.9 Hz, 1H), 8.22 (d, *J* = 8.3 Hz, 1H), 7.82 (t, *J* = 6.6 Hz, 1H), 7.56–7.49 (m, 1H), 7.30 (dt, *J* = 7.6, 3.1 Hz, 1H), 7.21–7.13 (m, 2H), 4.63–4.51 (m, 2H), 3.54 (q, *J* = 5.7 Hz, 2H), 2.91 (d, *J* = 3.8 Hz, 6H), 2.42 (s, 3H). MS: 323.1 [M + H]<sup>+</sup>. HRMS (MALDI) (*m/z*): [M + H]<sup>+</sup> calcd for C<sub>18</sub>H<sub>22</sub>N<sub>6</sub> + H<sup>+</sup>, 323.19850; found, 323.19750.

**4-(2-(Dimethylamino)ethoxy)picolinonitrile (12).** 2-(Dimethylamino)ethan-1-ol (289  $\mu$ L, 2.89 mmol, 1 equiv) was added dropwise to a mixture of NaH (60% dispersion) (138 mg, 3.46 mmol, 1.2 equiv) in DMF (12 mL) at 0  $^{\circ}$ C. The solution was allowed to warm to room temperature, and 4-chloropicolinonitrile (400 mg, 2.89 mmol, 1 equiv) was added. The reaction was stirred overnight at room temperature and poured over water. The resultant mixture was diluted in brine and extracted 3 $\times$  with EtOAc. The combined organics were washed with brine, dried over Na<sub>2</sub>SO<sub>4</sub>, filtered, and concentrated. The crude product was purified by silica gel chromatography (50% EtOAc/Hex  $\rightarrow$  EtOAc  $\rightarrow$  (5% MeOH, 2% TEA)/DCM) to give 4-(2-(dimethylamino)ethoxy)picolinonitrile (12) (295 mg, 1.54 mmol, 53% yield) as a light yellow oil.

**1-(4-(2-(Dimethylamino)ethoxy)pyridin-2-yl)ethan-1-one (13).** 4-(2-(Dimethylamino)ethoxy)picolinonitrile (12) (295 mg, 1.54 mmol, 1 equiv) was dissolved in THF (3 mL) and cooled to 0  $^{\circ}$ C under N<sub>2</sub>. MeMgI (3 M in Et<sub>2</sub>O) (770  $\mu$ L, 2.32 mmol, 1.5 equiv) was added dropwise, and the reaction was continuously stirred at 0  $^{\circ}$ C until complete by LC–MS. Water (5 mL) was added to quench the reaction followed by acidification to pH = 1 with 1 M HCl(aq). The mixture was stirred for 20 min, and the aqueous was subsequently washed with EtOAc to remove nonbasic impurities. The aqueous was basified to pH = 10 with 1 M NaOH and extracted 3 $\times$  with EtOAc. The combined organics were dried over Na<sub>2</sub>SO<sub>4</sub>, filtered, and concentrated to give 1-(4-(2-(dimethylamino)ethoxy)pyridin-2-yl)ethan-1-one (13) (288 mg) as a yellow oil that was carried on crude without further purification.

**(E)-2-((2-(1-(2-(Benzo[d]thiazol-2-yl)hydrazineylidene)ethyl)pyridin-4-yl)oxy)-N,N-dimethylethan-1-amine HCl (C28).** To a solution of 1-(4-(2-(dimethylamino)ethoxy)pyridin-2-yl)ethan-1-one (13) (120 mg, 0.576 mmol, 1 equiv) and 2-hydrazineylbenzo[d]thiazole (105 mg, 0.634 mmol, 1.1 equiv) in EtOH (5 mL) was added AcOH (3 drops). The reaction was stirred overnight at room temperature, determined complete by TLC, and concentrated under reduced pressure. Purification by silica gel chromatography (EtOAc  $\rightarrow$  (5% MeOH, 2% TEA)/DCM) gave the free base of C28 as a yellow oil. The yellow oil was dissolved in MeOH and acidified with HCl (2 M in Et<sub>2</sub>O) (excess). The solution was concentrated and recrystallized in MeOH/Et<sub>2</sub>O, and subsequently, the solid was filtered and dried under vacuum to give the title compound (E)-2-((2-(1-(2-(benzo[d]thiazol-2-yl)hydrazineylidene)ethyl)pyridin-4-yl)oxy)-N,N-dimethylethan-1-amine HCl (C28) (58.2 mg, 0.136 mmol, 98% purity by HPLC) as a light yellow solid. <sup>1</sup>H NMR (HCl salt) (500 MHz, methanol-*d*<sub>4</sub>):  $\delta$  8.69 (d, *J* = 6.9 Hz, 1H), 7.82 (d, *J* = 2.6 Hz,

1H), 7.71–7.65 (m, 1H), 7.55 (dd,  $J = 6.9$ , 2.6 Hz, 1H), 7.46 (d,  $J = 8.1$  Hz, 1H), 7.43–7.37 (m, 1H), 7.24 (td,  $J = 7.6$ , 1.2 Hz, 1H), 4.84–4.83 (m, 2H), 3.82–3.70 (m, 2H), 3.06 (s, 6H), 2.53 (s, 3H). MS: 356.1  $[M + H]^+$ . HRMS (MALDI) ( $m/z$ ):  $[M + H]^+$  calcd for  $C_{18}H_{21}N_3OS + H^+$ , 356.15450; found, 356.15400.

(*E*)-2-((2-(1-(2-(Benzo[d]oxazol-2-yl)hydrazineylidene)ethyl)pyridin-4-yl)oxy)-*N,N*-dimethylethan-1-amine HCl (**C35**). To a solution of 1-(4-(2-(dimethylamino)ethoxy)pyridin-2-yl)ethan-1-one (**13**) (60 mg, 0.29 mmol, 1 equiv) and 2-hydrazinylbenzo[d]oxazole (45 mg, 0.32 mmol, 1.1 equiv) in MeOH (3 mL) was added AcOH (3 drops). Purification by silica gel chromatography (5% MeOH/DCM  $\rightarrow$  5% MeOH, 5% TEA)/DCM gave the free base of **C35** as a yellow oil. The yellow oil was dissolved in MeOH and acidified with HCl (2 M in Et<sub>2</sub>O) (excess). The solution was concentrated and recrystallized in MeOH/Et<sub>2</sub>O, and subsequently, the solid was filtered and dried under vacuum to give the title compound (*E*)-2-((2-(1-(2-(benzo[d]oxazol-2-yl)hydrazineylidene)ethyl)pyridin-4-yl)oxy)-*N,N*-dimethylethan-1-amine HCl (**C35**) (31 mg, 0.075 mmol, 100% purity by HPLC) as a bright yellow solid. <sup>1</sup>H NMR (HCl salt) (500 MHz, methanol-*d*<sub>4</sub>):  $\delta$  8.75 (d,  $J = 6.8$  Hz, 1H), 7.84 (d,  $J = 2.6$  Hz, 1H), 7.56 (dd,  $J = 6.8$ , 2.6 Hz, 1H), 7.51–7.44 (m, 2H), 7.34 (td,  $J = 7.7$ , 1.1 Hz, 1H), 7.26 (td,  $J = 7.8$ , 1.3 Hz, 1H), 4.85–4.82 (m, 2H), 3.82–3.74 (m, 2H), 3.06 (s, 6H), 2.50 (s, 3H). MS: 339.8  $[M + H]^+$ . HRMS (MALDI) ( $m/z$ ):  $[2M + H]^+$  calcd for  $(C_{18}H_{21}N_3O_2)_2 + H^+$ , 679.34390; found, 679.34630.

4-(2-(2-Chloro-1H-benzo[d]imidazol-1-yl)ethyl)morpholine (**14**). To a solution of 2-chloro-1H-benzo[d]imidazole (2.47 g, 16.2 mmol, 1 equiv) in DMF (35 mL) at 0 °C was added NaH (60% dispersion) (1.94 g, 24.3 mmol, 3 equiv) in multiple portions. After stirring for 10 min at 0 °C, 4-(2-chloroethyl)morpholine (3.5 g, 24.3 mmol, 1.5 equiv) was added and the reaction was allowed to stir overnight as it slowly warmed to room temperature. The reaction proceeded to roughly 80% completion by LC–MS but was quenched with water and partitioned in EtOAc/H<sub>2</sub>O. The organic was washed 2 $\times$  with water and 1 $\times$  with brine, dried over Na<sub>2</sub>SO<sub>4</sub>, filtered, and concentrated. The residue was purified by silica gel chromatography (50% EtOAc/Hex  $\rightarrow$  EtOAc), and product containing fractions were concentrated to give 4-(2-(2-chloro-1H-benzo[d]imidazol-1-yl)ethyl)morpholine (**14**) (3.57 g, 13.4 mmol) as a viscous pink oil that was dried under high vacuum and used without further purification in the subsequent reaction. MS: 265.9  $[M + H]^+$ .

4-(2-(2-Hydrazineyl-1H-benzo[d]imidazol-1-yl)ethyl)morpholine (**15**). To a solution of 4-(2-(2-chloro-1H-benzo[d]imidazol-1-yl)ethyl)morpholine (**14**) (3.5 g, 13.2 mmol) in ethylene glycol (10 mL) was added hydrazine hydrate (2 mL). The reaction was heated for 2 h at 140 °C and was determined complete by TLC (5% MeOH/DCM). The reaction was concentrated under reduced pressure, redissolved in *i*-PrOH, and reconstituted 4 $\times$  to remove excess hydrazine. The title compound 4-(2-(2-hydrazineyl-1H-benzo[d]imidazol-1-yl)ethyl)morpholine (**15**) in 10 mL ethylene glycol was used as is in the next reaction, assuming quantitative yield. MS: 261.9  $[M + H]^+$ .

(*E*)-4-(2-(2-(2-(1-(Pyridin-2-yl)ethylidene)hydrazineyl)-1H-benzo[d]imidazol-1-yl)ethyl)morpholine HCl (**C42**). To a solution of 4-(2-(2-hydrazineyl-1H-benzo[d]imidazol-1-yl)ethyl)morpholine (**15**) (crude from the previous reaction) in EtOH (10 mL) and ethylene glycol (10 mL, remaining from the previous reaction) was added 1-(pyridin-2-yl)ethan-1-one (2 mL, 17.6 mmol, 1.33 equiv) followed by AcOH (20 drops). The reaction was stirred overnight at room temperature, determined complete by LC–MS, and concentrated under reduced pressure. The crude reaction was partitioned in DCM/NaHCO<sub>3</sub>(sat, aq), and the aqueous was extracted 3 $\times$  with DCM. The combined organic was dried over Na<sub>2</sub>SO<sub>4</sub>, filtered, and concentrated. The residue was purified by basic alumina chromatography (50% EtOAc/Hex  $\rightarrow$  EtOAc), and product fractions were concentrated and repurified by silica gel chromatography (EtOAc  $\rightarrow$  2% MeOH/EtOAc) to give the title compound (*E*)-4-(2-(2-(2-(1-(pyridin-2-yl)ethylidene)hydrazineyl)-1H-benzo[d]imidazol-1-yl)ethyl)morpholine (**C42**) (1.51 g, free base) as an orange foam. This foam was dissolved in MeOH (20 mL), acidified with HCl (2 M in Et<sub>2</sub>O) (7 mL), and concentrated under reduced pressure. The concentrate

was recrystallized from MeOH/Et<sub>2</sub>O, filtered, and dried under vacuum to give (*E*)-4-(2-(2-(2-(1-(pyridin-2-yl)ethylidene)hydrazineyl)-1H-benzo[d]imidazol-1-yl)ethyl)morpholine HCl (**C42**) (1.78 g, 4.07 mmol, 100% purity by HPLC) as a light orange solid. <sup>1</sup>H NMR (HCl salt) (400 MHz, methanol-*d*<sub>4</sub>):  $\delta$  8.79 (ddd,  $J = 5.9$ , 1.6, 0.7 Hz, 1H), 8.61 (ddd,  $J = 8.2$ , 7.7, 1.6 Hz, 1H), 8.32–8.27 (m, 1H), 7.94 (ddd,  $J = 7.6$ , 5.8, 1.1 Hz, 1H), 7.55 (dd,  $J = 5.9$ , 3.2 Hz, 1H), 7.48–7.42 (m, 1H), 7.28 (dd,  $J = 5.9$ , 3.1 Hz, 2H), 4.81 (t,  $J = 6.4$  Hz, 2H), 3.97 (s, 4H), 3.76 (t,  $J = 6.4$  Hz, 2H), 3.59 (s, 4H), 2.57 (s, 3H). MS: 365.15  $[M + H]^+$ . HRMS (MALDI) ( $m/z$ ):  $[M + H]^+$  calcd for  $C_{20}H_{24}N_6O + H^+$ , 365.20880; found, 365.20840.

4-(2-((Tetrahydro-2H-pyran-2-yl)oxy)ethoxy)picolinonitrile (**16**). To a solution of NaH (60% dispersion) (1.04 g, 26 mmol, 1.2 equiv) in DMF (50 mL) at 0 °C was added 2-((tetrahydro-2H-pyran-2-yl)oxy)ethan-1-ol (3.16 g, 21.7 mmol, 1 equiv). The solution was allowed to warm to room temperature and stirred for 1 h. 4-Chloropicolinonitrile (3.0 g, 21.7 mmol, 1 equiv) was added, and the reaction was allowed to stir overnight at room temperature. The resultant mixture was diluted in brine and extracted 3 $\times$  with EtOAc. The combined organics were washed 1 $\times$  with water and 3 $\times$  with brine, dried over Na<sub>2</sub>SO<sub>4</sub>, filtered, and concentrated. The crude product was purified by silica gel chromatography (35%  $\rightarrow$  65% EtOAc/Hex) to give 4-(2-((tetrahydro-2H-pyran-2-yl)oxy)ethoxy)picolinonitrile (**16**) (3.33 g, 13.4 mmol, 62% yield) as a yellow oil.

1-(4-(2-Hydroxyethoxy)pyridin-2-yl)ethan-1-one (**17**). 4-(2-((Tetrahydro-2H-pyran-2-yl)oxy)ethoxy)picolinonitrile (**16**) (248 mg, 1.0 mmol, 1 equiv) was dissolved in THF (2 mL) and cooled to 0 °C under N<sub>2</sub>. MeMgI (3 M in Et<sub>2</sub>O) (500  $\mu$ L, 1.5 mmol, 1.5 equiv) was added dropwise, and the reaction was allowed to warm to room temperature. After 3 h, the reaction was determined complete by LC–MS, quenched with water (5 mL), and acidified to pH = 1 with 1 M HCl(aq). The mixture was stirred for 2 h to give complete deprotection of the THP protecting group in situ. The mixture was basified to pH = 7 with 1 M NaOH and extracted 3 $\times$  with EtOAc. The combined organics were dried over Na<sub>2</sub>SO<sub>4</sub>, filtered, and concentrated to give 1-(4-(2-hydroxyethoxy)pyridin-2-yl)ethan-1-one (**17**) (154 mg) as an oil that was carried on crude without further purification.

(*E*)-2-((2-(1-(2-(Benzo[d]thiazol-2-yl)hydrazineylidene)ethyl)pyridin-4-yl)oxy)ethan-1-ol (**C61**). To a solution of 1-(4-(2-hydroxyethoxy)pyridin-2-yl)ethan-1-one (**17**) (150 mg, 0.83 mmol, 1 equiv) and 2-hydrazinylbenzo[d]thiazole (137 mg, 0.83 mmol, 1 equiv) in DCM (2 mL) and MeOH (2 mL) was added AcOH (4 drops). The reaction was stirred overnight, determined complete by LC–MS, and concentrated under reduced pressure. The residual solid was recrystallized from MeOH to give the title compound (*E*)-2-((2-(1-(2-(benzo[d]thiazol-2-yl)hydrazineylidene)ethyl)pyridin-4-yl)oxy)ethan-1-ol (**C61**) (71 mg, 0.22 mmol, 99.1% purity by HPLC) as a white solid. <sup>1</sup>H NMR (500 MHz, methanol-*d*<sub>4</sub>):  $\delta$  8.38 (d,  $J = 5.8$  Hz, 1H), 7.76 (d,  $J = 2.4$  Hz, 1H), 7.72 (s, 1H), 7.54 (s, 1H), 7.39–7.29 (br. m, 1H), 7.17 (br. m, 1H), 7.01 (dd,  $J = 5.8$ , 2.6 Hz, 1H), 4.29–4.22 (m, 2H), 4.01–3.94 (m, 2H), 2.45 (s, 3H). MS: 328.9  $[M + H]^+$ .

2-((2-Acetylpyridin-4-yl)oxy)ethyl Methanesulfonate (**18**). To a solution of 1-(4-(2-hydroxyethoxy)pyridin-2-yl)ethan-1-one (**17**) (933 mg, 5.15 mmol, 1 equiv) in DCM (20 mL) was added TEA (1.08 mL, 7.7 mmol, 1.5 equiv) followed by methanesulfonyl chloride (dropwise) (600  $\mu$ L, 7.7 mmol, 1.5 equiv). After stirring for 2 h at room temperature, the reaction was quenched with NaHCO<sub>3</sub>(sat, aq) and partitioned in EtOAc/H<sub>2</sub>O. The aqueous was extracted 3 $\times$  with EtOAc, and the combined organics were washed 1 $\times$  with brine, dried over Na<sub>2</sub>SO<sub>4</sub>, filtered, and concentrated to give 2-((2-acetylpyridin-4-yl)oxy)ethyl methanesulfonate (**18**) (1.16 g) as a brown oil that solidified on standing. This product was used without further purification in subsequent reactions.

1-(4-(2-(4-Methylpiperazin-1-yl)ethoxy)pyridin-2-yl)ethan-1-one (**19**). To a solution of 2-((2-acetylpyridin-4-yl)oxy)ethyl methanesulfonate (**18**) (200 mg, 0.77 mmol, 1 equiv) in MeCN (15 mL) was added 1-methylpiperazine (171  $\mu$ L, 1.54 mmol, 2 equiv) followed by KI (128 mg, 0.77 mmol, 1 equiv) and K<sub>2</sub>CO<sub>3</sub> (213 mg, 1.54 mmol, 2



equiv). After heating for 6 h at 80 °C, the reaction was determined complete by LC–MS, cooled to room temperature, and poured into water. The resulting mixture was extracted 3× with EtOAc, and the combined organics were dried over Na<sub>2</sub>SO<sub>4</sub>, filtered, and concentrated to give 1-(4-(2-(4-methylpiperazin-1-yl)ethoxy)pyridin-2-yl)ethan-1-one (**19**) (145 mg, 0.55 mmol) as a pale orange oil that was used crude without further purification.

(*E*)-2-(2-(1-(4-(2-(4-methylpiperazin-1-yl)ethoxy)pyridin-2-yl)ethylidene)hydrazineyl)benzo[d]thiazole HCl (**C64**). To a solution of 1-(4-(2-(4-methylpiperazin-1-yl)ethoxy)pyridin-2-yl)ethan-1-one (**19**) (145 mg, 0.55 mmol, 1 equiv) in DCM (2 mL) and MeOH (2 mL) was added 2-hydrazinylbenzo[d]thiazole (91 mg, 0.55 mmol, 1 equiv). AcOH (4 drops) was added, and the reaction was stirred overnight at room temperature. The reaction was determined complete by LC–MS and concentrated under reduced pressure. The product was redissolved in MeOH and neutralized with TEA (0.1 mL) in order to generate the free base for column chromatography. After concentration, the product was purified by silica gel chromatography (2% MeOH/DCM → (5% MeOH, 2% TEA)/DCM). Product containing fractions were concentrated under reduced pressure. The residue was redissolved in MeOH and converted to the HCl salt with the addition of 2 M HCl/Et<sub>2</sub>O (1 mL). The mixture was concentrated and recrystallized from MeOH to afford the title compound (*E*)-2-(2-(1-(4-(2-(4-methylpiperazin-1-yl)ethoxy)pyridin-2-yl)ethylidene)hydrazineyl)benzo[d]thiazole HCl (**C64**) (73 mg, 0.15 mmol, 98.9% purity by HPLC) as a yellow solid. <sup>1</sup>H NMR (500 MHz, deuterium oxide): δ 8.41 (d, *J* = 6.9 Hz, 1H), 7.60 (d, *J* = 8.3 Hz, 1H), 7.44 (d, *J* = 2.6 Hz, 1H), 7.38 (d, *J* = 7.8 Hz, 1H), 7.30 (ddd, *J* = 8.3, 7.4, 1.2 Hz, 1H), 7.27 (dd, *J* = 7.0, 2.7 Hz, 1H), 7.16–7.12 (m, 1H), 4.51–4.47 (m, 2H), 3.37 (br. s, 4H), 3.27–3.23 (m, 2H), 3.13 (br. s, 4H), 2.84 (s, 3H), 2.28 (s, 3H). MS: 411.1 [M + H]<sup>+</sup>.

2-Bromo-1-(pyridin-2-yl)ethan-1-one HBr (**20**). 1-(Pyridin-2-yl)ethan-1-one (930 μL, 8.25 mmol, 1 equiv) was dissolved in a mixture of HBr (33%, aq) (1.4 mL) and AcOH (3.7 mL). A pyridinium salt quickly precipitated from solution. To this mixture under vigorous stirring was added a mixture of Br<sub>2</sub> (0.42 mL, 8.25 mmol, 1 equiv) in AcOH (0.92 mL). After stirring overnight at room temperature, the reaction was diluted in Et<sub>2</sub>O and the precipitated solid was filtered and washed with additional Et<sub>2</sub>O. Drying the solid under high vacuum yielded 2-bromo-1-(pyridin-2-yl)ethan-1-one (**20**) (2.26 g, HBr salt, 8.1 mmol) as a white solid.

(*Z*)-2-(2-(2-Methoxy-1-(pyridin-2-yl)ethylidene)hydrazineyl)benzo[d]thiazole (**C65**). To a mixture of 2-bromo-1-(pyridin-2-yl)ethan-1-one HBr (**20**) (281 mg, 1 mmol, 1 equiv) and 2-hydrazinylbenzo[d]thiazole (165 mg, 1 mmol, 1 equiv) in DCM (4 mL) and MeOH (2 mL) was added AcOH (4 drops). The reaction was stirred overnight at room temperature and determined complete by LC–MS. The orange precipitate was filtered, subsequently recrystallized from MeOH, filtered, washed with MeOH, and dried under vacuum to give (*Z*)-2-(2-(2-methoxy-1-(pyridin-2-yl)ethylidene)hydrazineyl)benzo[d]thiazole (**C65**) (47 mg, 0.16 mmol, 97.1% purity by HPLC) as an orange solid. <sup>1</sup>H NMR (400 MHz, methanol-*d*<sub>4</sub>): δ 8.77 (ddd, *J* = 5.9, 1.6, 0.7 Hz, 1H), 8.60 (ddd, *J* = 8.3, 7.6, 1.6 Hz, 1H), 8.45 (ddd, *J* = 8.3, 1.2, 0.8 Hz, 1H), 7.97 (ddd, *J* = 7.5, 5.9, 1.3 Hz, 1H), 7.70–7.62 (m, 1H), 7.43–7.35 (m, 2H), 7.24 (ddd, *J* = 7.9, 6.8, 1.7 Hz, 1H), 4.96 (s, 2H), 3.47 (s, 3H). MS: 298.85 [M + H]<sup>+</sup>.

1-(2-(Pyrrolidin-1-yl)ethyl)-1H-benzo[d]imidazole (**21**). To a solution of 1H-benzo[d]imidazole (3.0 g, 25.4 mmol, 1 equiv) in DMF (30 mL) was added 1-(2-chloroethyl)pyrrolidine HCl (6.48 g, 38.1 mmol, 1.5 equiv) followed by K<sub>2</sub>CO<sub>3</sub> (10.5 g, 76.2 mmol, 3 equiv). After stirring for 2 h at 60 °C, the reaction was determined complete by TLC (10% MeOH/DCM). The reaction was partitioned in EtOAc/H<sub>2</sub>O, and the organic was washed 3× H<sub>2</sub>O and 1× brine, dried over Na<sub>2</sub>SO<sub>4</sub>, filtered, and concentrated. Silica gel chromatography (5% → 10% MeOH/DCM) yielded 1-(2-(pyrrolidin-1-yl)ethyl)-1H-benzo[d]imidazole (**21**) (2.94 g, 13.7 mmol) after concentration of product fractions. MS: 215.95 [M + H]<sup>+</sup>.

Di-*tert*-butyl 1-(1-(2-(Pyrrolidin-1-yl)ethyl)-1H-benzo[d]imidazol-2-yl)hydrazine-1,2-dicarboxylate (**22**). To a solution of 1-(2-(pyrrolidin-1-yl)ethyl)-1H-benzo[d]imidazole (**21**) (1.70 g, 7.9 mmol, 1 equiv) in THF (25 mL) at –78 °C was added *n*-BuLi (2.5 M in hexanes) (3.5 mL, 8.7 mmol, 1.1 equiv) dropwise over 10 min. After stirring for 10 min at –78 °C, a solution of di-*tert*-butyl-azodicarboxylate (2.0 g, 8.7 mmol, 1.1 equiv) in THF (7 mL) was added dropwise over 10 min. After stirring for an additional 10 min at –78 °C, the reaction was allowed to warm to room temperature and was stirred for an additional 30 min. The reaction was observed as approximately 90% complete by LC–MS and was quenched with H<sub>2</sub>O. The mixture was partitioned in EtOAc/H<sub>2</sub>O, and the organic was washed 2× with H<sub>2</sub>O and 1× with brine, dried over Na<sub>2</sub>SO<sub>4</sub>, filtered, and concentrated. The residue was purified by silica gel chromatography (50% EtOAc/Hex → EtOAc), and product containing fractions were concentrated to give di-*tert*-butyl 1-(1-(2-(pyrrolidin-1-yl)ethyl)-1H-benzo[d]imidazol-2-yl)hydrazine-1,2-dicarboxylate (**22**) (2.35 g, 5.3 mmol) as an orange solid. MS: 446.15 [M + H]<sup>+</sup>.

(*E*)-2-(2-(1-(Pyridin-2-yl)ethylidene)hydrazineyl)-1-(2-(pyrrolidin-1-yl)ethyl)-1H-benzo[d]imidazole HCl (**C69**). To a solution of di-*tert*-butyl 1-(1-(2-(pyrrolidin-1-yl)ethyl)-1H-benzo[d]imidazol-2-yl)hydrazine-1,2-dicarboxylate (**22**) in MeOH (30 mL) was added 1-(pyridin-2-yl)ethan-1-one (591 μL, 5.27 mmol, 1 equiv). HCl (4 M in dioxane) (8 mL) was added, and the reaction was stirred overnight at room temperature. The reaction was determined complete by LC–MS, and the precipitated solid was filtered. The filtrate was concentrated and recrystallized from *i*-PrOH to collect a second crop of solid. The combined solids were recrystallized from MeOH/EtOAc, sonicated, and filtered. The solid was dried under high vacuum to afford (*E*)-2-(2-(1-(pyridin-2-yl)ethylidene)hydrazineyl)-1-(2-(pyrrolidin-1-yl)ethyl)-1H-benzo[d]imidazole HCl (**C69**) (1.35 g, 3.2 mmol, 98.4% purity by HPLC) as a light orange solid. <sup>1</sup>H NMR (500 MHz, methanol-*d*<sub>4</sub>): δ 8.80 (ddd, *J* = 5.8, 1.6, 0.6 Hz, 1H), 8.62 (ddd, *J* = 8.3, 7.7, 1.6 Hz, 1H), 8.31 (d, *J* = 8.3 Hz, 1H), 7.95 (ddd, *J* = 7.5, 5.8, 1.1 Hz, 1H), 7.58–7.53 (m, 1H), 7.49–7.44 (m, 1H), 7.34–7.28 (m, 2H), 4.75 (t, *J* = 6.3 Hz, 2H), 3.89 (s, 2H), 3.81 (t, *J* = 6.3 Hz, 2H), 3.27 (s, 2H), 2.60 (s, 3H), 2.21 (s, 2H), 2.04 (s, 2H). MS: 348.95 [M + H]<sup>+</sup>. HRMS (MALDI) (*m/z*): [M + H]<sup>+</sup> calcd for C<sub>20</sub>H<sub>24</sub>N<sub>6</sub> + H<sup>+</sup>, 349.21410; found, 349.21350.

(*E*)-2-(2-(1-(Pyrimidin-2-yl)ethylidene)hydrazineyl)benzo[d]thiazole AcOH (**C77**). To a solution of 1-(pyrimidin-2-yl)ethan-1-one (74 mg, 0.61 mmol, 1 equiv) and 2-hydrazinylbenzo[d]thiazole (100 mg, 0.61 mmol, 1 equiv) in MeOH (5 mL) was added AcOH (5 drops). The reaction was stirred overnight at room temperature, and the precipitated solid was filtered, washed with MeOH, and dried under high vacuum to afford (*E*)-2-(2-(1-(pyrimidin-2-yl)ethylidene)hydrazineyl)benzo[d]thiazole AcOH (**C77**) (47.6 mg, 0.15 mmol, 98.9% purity by HPLC) as a light brown solid. <sup>1</sup>H NMR (acetate salt) (500 MHz, DMSO-*d*<sub>6</sub>): δ 11.92 (s, 2H), 8.89 (d, *J* = 4.8 Hz, 2H), 7.77 (d, *J* = 7.8 Hz, 1H), 7.47 (t, *J* = 4.8 Hz, 1H), 7.44 (d, *J* = 7.8 Hz, 1H), 7.36–7.27 (m, 1H), 7.17–7.10 (m, 1H), 2.45 (s, 3H), 1.91 (s, 3H, acetate CH<sub>3</sub>). MS: 330.0 [M + H]<sup>+</sup>. HRMS (MALDI) (*m/z*): [2M + H]<sup>+</sup> calcd for (C<sub>13</sub>H<sub>11</sub>N<sub>5</sub>S)<sub>2</sub> + H<sup>+</sup>, 539.15310; found, 539.15430.

Di-*tert*-butyl 1-(1-Methyl-1H-imidazol-2-yl)hydrazine-1,2-dicarboxylate (**23**). To a solution of 1-methyl-1H-imidazole (**1**) (1.0 g, 12.2 mmol, 1 equiv) in THF (10 mL) at –78 °C was added *n*-BuLi (2.5 M in hexanes, 5.4 mL, 13.4 mmol, 1.1 equiv). After stirring for 10 min at –78 °C, a solution of di-*tert*-butyl-azodicarboxylate (3.09 g, 13.4 mmol, 1.1 equiv) in THF (5 mL) was added dropwise over 5 min. The reaction was allowed to stir for 30 min at –78 °C before being warmed to room temperature and quenched with water. The reaction was diluted in EtOAc, washed 1× with water and 1× with brine, dried over Na<sub>2</sub>SO<sub>4</sub>, filtered, and concentrated. The crude mixture was purified by silica gel chromatography, eluting in 50% → 75% EtOAc/Hex. Product containing fractions were combined and concentrated to afford the title compound di-*tert*-butyl 1-(1-methyl-1H-imidazol-2-yl)hydrazine-1,2-dicarboxylate (**23**) (1.54 g, 40% yield) as a white crystalline solid. MS: 313.1 [M + H]<sup>+</sup>.



2-(1-(2-(1-Methyl-1H-imidazol-2-yl)hydrazono)ethyl)pyridine HCl (**C78**). Di-*tert*-butyl 1-(1-methyl-1H-imidazol-2-yl)hydrazine-1,2-dicarboxylate (**23**) (800 mg, 2.56 mmol, 1 equiv) and 1-(pyridin-2-yl)ethan-1-one (287  $\mu$ L, 2.56 mmol, 1 equiv) were dissolved in MeOH (15 mL). Following addition of 4 N HCl/dioxane (4.0 mL, 16.0 mmol, 6.25 equiv), the reaction was allowed to stir for 16 h at room temperature. The crude reaction mixture was concentrated and recrystallized from a mixture of MeOH and EtOAc to give the title compound 2-(1-(2-(1-methyl-1H-imidazol-2-yl)hydrazono)ethyl)pyridine HCl (**C78**) (571 mg, 2.27 mmol, 100% purity by HPLC) as a yellow solid.  $^1\text{H}$  NMR (400 MHz, methanol- $d_4$ ):  $\delta$  8.91 (ddd,  $J$  = 5.8, 1.6, 0.7 Hz, 1H), 8.69 (td,  $J$  = 8.0, 1.6 Hz, 1H), 8.47 (dt,  $J$  = 8.2, 0.9 Hz, 1H), 8.08 (ddd,  $J$  = 7.7, 5.7, 1.2 Hz, 1H), 7.28 (d,  $J$  = 2.3 Hz, 1H), 7.23 (d,  $J$  = 2.3 Hz, 1H), 3.82 (s, 3H), 2.62 (s, 3H). MS: 216.15  $[M + H]^+$ . HRMS (MALDI) ( $m/z$ ):  $[2M + H]^+$  calcd for  $(C_{11}H_{13}N_5)_2 + H^+$ , 431.24180; found, 431.24150.

2-(1H-Benzo[d]imidazol-1-yl)-1-(3,3-difluoropyrrolidin-1-yl)ethan-1-one (**24**). A mixture of 1H-benzo[d]imidazole (514 mg, 4.35 mmol, 1 equiv), 2-chloro-1-(3,3-difluoropyrrolidin-1-yl)ethan-1-one (800 mg, 4.35 mmol, 1 equiv), and  $K_2CO_3$  (1.2 g, 8.7 mmol, 2 equiv) in DMF (15 mL) was stirred overnight at 60  $^\circ\text{C}$ . The reaction was determined complete by LC–MS and partitioned in EtOAc/ $H_2O$ . The aqueous was extracted 2 $\times$  with EtOAc, and the combined organic was dried over  $Na_2SO_4$ , filtered, and concentrated. The residue was purified by silica gel chromatography (EtOAc  $\rightarrow$  2% MeOH/EtOAc  $\rightarrow$  5% MeOH/EtOAc) to afford 2-(1H-benzo[d]imidazol-1-yl)-1-(3,3-difluoropyrrolidin-1-yl)ethan-1-one (**24**) (705 mg, 2.7 mmol) as a white solid after concentration. MS: 265.65  $[M + H]^+$ .

1-(2-(3,3-Difluoropyrrolidin-1-yl)ethyl)-1H-benzo[d]imidazole (**25**). To a solution of 2-(1H-benzo[d]imidazol-1-yl)-1-(3,3-difluoropyrrolidin-1-yl)ethan-1-one (**24**) (400 mg, 1.5 mmol, 1 equiv) in THF (10 mL) was added  $BH_3 \cdot THF$  (2 M in THF) (2.25 mL, 4.5 mmol, 3 equiv). After stirring overnight at room temperature, the reaction was 1/3 complete by LC–MS. Additional  $BH_3 \cdot THF$  (2 M in THF) (5.0 mL, 10 mmol, 6.7 equiv) was added, and the reaction was determined complete after 4 h at room temperature. MeOH (10 mL) and HCl (4 M in dioxane) (10 mL) were added, and the reaction was stirred overnight. The mixture was concentrated and partitioned in EtOAc/ $H_2O$ . The product was partitioned into the mildly acidic aqueous, and the organic was extracted 2 $\times$  with water. The combined aqueous was neutralized with  $NaHCO_3$  (sat, aq) and extracted 3 $\times$  with DCM. The combined organics were dried over  $Na_2SO_4$ , filtered, and concentrated. The crude product was purified by silica gel chromatography (50% EtOAc/Hex  $\rightarrow$  EtOAc), and product fractions were concentrated to give 1-(2-(3,3-difluoropyrrolidin-1-yl)ethyl)-1H-benzo[d]imidazole (**25**) (273 mg, 1.09 mmol) as a white crystalline solid. MS: 251.70  $[M + H]^+$ .

Di-*tert*-butyl 1-(1-(2-(3,3-Difluoropyrrolidin-1-yl)ethyl)-1H-benzo[d]imidazol-2-yl)hydrazine-1,2-dicarboxylate (**26**). To a solution of 1-(2-(3,3-difluoropyrrolidin-1-yl)ethyl)-1H-benzo[d]imidazole (**25**) (270 mg, 1.07 mmol, 1 equiv) in THF (10 mL) at  $-78^\circ\text{C}$  was added *n*-BuLi (2.5 M in hexanes) (472  $\mu$ L, 1.18 mmol, 1.1 equiv). After 5 min at  $-78^\circ\text{C}$ , di-*tert*-butyl-azodicarboxylate (272 mg, 1.18 mmol, 1.1 equiv) in THF (2 mL) was added and the reaction was stirred for 30 min at  $-78^\circ\text{C}$  before slowly warming to room temperature and stirring overnight. The reaction was complete by LC–MS, quenched with water, and partitioned in EtOAc/ $H_2O$ . The organic was washed 1 $\times$  with water and 1 $\times$  with brine, dried over  $Na_2SO_4$ , filtered, and concentrated. Purification by silica gel chromatography (25% EtOAc/Hex) afforded di-*tert*-butyl 1-(1-(2-(3,3-difluoropyrrolidin-1-yl)ethyl)-1H-benzo[d]imidazol-2-yl)hydrazine-1,2-dicarboxylate (**26**) (267 mg, 0.56 mmol) as a white solid after concentration. MS: 482.1  $[M + H]^+$ .

(*E*)-1-(2-(3,3-Difluoropyrrolidin-1-yl)ethyl)-2-(2-(1-(pyridin-2-yl)ethylidene)hydrazineyl)-1H-benzo[d]imidazole HCl (**C85**). To a solution of di-*tert*-butyl 1-(1-(2-(3,3-difluoropyrrolidin-1-yl)ethyl)-1H-benzo[d]imidazol-2-yl)hydrazine-1,2-dicarboxylate (**26**) (150 mg, 0.31 mmol, 1 equiv) and 1-(pyridin-2-yl)ethan-1-one (35  $\mu$ L, 0.31 mmol, 1 equiv) in MeOH (2 mL) was added HCl (4 M in dioxane)

(1 mL). After stirring for 1 h at 60  $^\circ\text{C}$ , the reaction was determined complete by LC–MS and cooled to room temperature. The precipitated solid was filtered, washed with MeOH, and dried under vacuum to give (*E*)-1-(2-(3,3-difluoropyrrolidin-1-yl)ethyl)-2-(2-(1-(pyridin-2-yl)ethylidene)hydrazineyl)-1H-benzo[d]imidazole HCl (**C85**) (137 mg, 0.30 mmol, 99.2% purity by HPLC) as a light orange solid.  $^1\text{H}$  NMR (400 MHz, methanol- $d_4$ ):  $\delta$  8.76 (ddd,  $J$  = 5.8, 1.6, 0.7 Hz, 1H), 8.60 (ddd,  $J$  = 8.3, 7.7, 1.6 Hz, 1H), 8.28 (dt,  $J$  = 8.3, 1.0 Hz, 1H), 7.91 (ddd,  $J$  = 7.6, 5.9, 1.2 Hz, 1H), 7.53–7.45 (m, 1H), 7.45–7.37 (m, 1H), 7.28–7.22 (m, 2H), 4.71 (t,  $J$  = 6.0 Hz, 2H), 4.27 (t,  $J$  = 11.6 Hz, 2H), 3.97–3.87 (m, 4H), 2.79–2.64 (m, 2H), 2.56 (s, 3H). MS: 384.80  $[M + H]^+$ . HRMS (MALDI) ( $m/z$ ):  $[M + H]^+$  calcd for  $C_{20}H_{22}F_2N_6 + H^+$ , 385.19520; found, 385.19470.

Di-*tert*-butyl 1-(1-(1-Methyl-1H-benzo[d]imidazol-2-yl)hydrazine-1,2-dicarboxylate (**27**). To a solution of 1-methyl-1H-benzo[d]imidazole (1.54 g, 11.6 mmol, 1 equiv) in THF (35 mL) at  $-78^\circ\text{C}$  was added *n*-BuLi (2.5 M in hexanes) (5.1 mL, 12.8 mmol, 1.1 equiv). After stirring for 15 min at  $-78^\circ\text{C}$ , a solution of di-*tert*-butyl-azodicarboxylate (2.95 g, 12.8 mmol, 1 equiv) in THF (11 mL) was added and the reaction was allowed to stir overnight while slowly warming to room temperature. The reaction was determined complete by LC–MS and poured into water. The resulting solution was extracted 3 $\times$  with EtOAc, and the combined organics were dried over  $Na_2SO_4$ , filtered, and concentrated. The brown residual oil was purified by silica gel chromatography (50% EtOAc/Hex) to give the title compound di-*tert*-butyl 1-(1-methyl-1H-benzo[d]imidazol-2-yl)hydrazine-1,2-dicarboxylate (**27**) (1.78 g, 4.9 mmol) as an orange oil after concentration of product fractions.

(*E*)-1-Methyl-2-(2-(1-(pyrimidin-2-yl)ethylidene)hydrazineyl)-1H-benzo[d]imidazole HCl (**C89**). To a mixture of di-*tert*-butyl 1-(1-methyl-1H-benzo[d]imidazol-2-yl)hydrazine-1,2-dicarboxylate (**27**) (100 mg, 0.82 mmol, 1 equiv) and 1-(pyrimidin-2-yl)ethan-1-one (297 mg, 0.82 mmol, 1 equiv) in MeOH (5 mL) was added HCl (4 M in dioxane) (1.25 mL, 4.9 mmol, 6 equiv). The mixture was stirred overnight and determined complete by LC–MS. The precipitated product was filtered, and the collected solid was recrystallized from MeOH/ $Et_2O$ . The recrystallized solid was filtered and dried under vacuum to yield the title compound (*E*)-1-methyl-2-(2-(1-(pyrimidin-2-yl)ethylidene)hydrazineyl)-1H-benzo[d]imidazole HCl (**C89**) (76.8 mg, 0.25 mmol, 99.3% purity) as a yellow solid.  $^1\text{H}$  NMR (400 MHz, DMSO- $d_6$ ):  $\delta$  9.08 (d,  $J$  = 5.1 Hz, 2H), 7.71 (t,  $J$  = 5.0 Hz, 1H), 7.58 (s, 1H), 7.46 (s, 1H), 7.33–7.29 (m, 2H), 3.82 (s, 3H), 2.53 (s, 3H). MS: 289.1  $[M + Na]^+$ . HRMS (MALDI) ( $m/z$ ):  $[2M + H]^+$  calcd for  $(C_{14}H_{14}N_6)_2 + H^+$ , 533.2629; found, 533.26330.

$Zn((E)-N'-(1-(pyridin-2-yl)ethylidene)azetidene-1-carbothiohydrazide)_2$  (**Zn-1**). To a suspension of (*E*)-*N'*-(1-(pyridin-2-yl)ethylidene)azetidene-1-carbothiohydrazide (**ZMC1**) (190.8 mg, 0.814 mmol, 1 equiv) in EtOH (20 mL) was added  $ZnCl_2$  (55.5 mg, 0.407 mmol, 0.5 equiv). After 5 min, TEA (0.80 mL, excess) was added and the mixture was heated for 2 h at reflux under nitrogen. Upon cooling to ambient temperature, a solid precipitate was collected by filtration and washed with EtOH followed by  $Et_2O$ . The solids were dried under high vacuum to give  $Zn((E)-N'-(1-(pyridin-2-yl)ethylidene)azetidene-1-carbothiohydrazide)_2$  (**Zn-1**) (215 mg, 0.404 mmol, 99%) as a bright yellow solid.  $^1\text{H}$  NMR (400 MHz, DMSO- $d_6$ ):  $\delta$  2.26 (overlapping tt,  $J$  = 7.48, 7.40 Hz, 4H), 2.58 (s, 6H), 4.05 (m, 8H), 7.29 (dd,  $J$  = 7.28, 5.60 Hz, 2H), 7.75 (m, 4H), 7.88 (dt,  $J$  = 8.04, 1.52 Hz, 2H). Slow evaporation of  $[Zn(ZMC1)_2]$  from a 1:1 mixture of DCM/MeOH afforded yellow crystals that were suitable for X-ray crystallography. HRMS (MALDI) ( $m/z$ ):  $[M + H]^+$  calcd for  $C_{22}H_{26}N_8S_2Zn + H^+$ , 531.10810; found, 531.10860.

$Zn((E)-2-(2-(1-(pyridin-2-yl)ethylidene)hydrazineyl)benzo[d]thiazole)_2$  (**Zn-2**). To a suspension of (*E*)-2-(2-(1-(pyridin-2-yl)ethylidene)hydrazineyl)benzo[d]thiazole (**C1**) (75.0 mg, 0.279 mmol, 1 equiv) in EtOH (7 mL) was added  $ZnCl_2$  (19.1 mg, 0.140 mmol, 0.5 equiv). After 5 min, TEA (0.279 mL, excess) was added and the mixture was heated for 2 h at reflux under nitrogen. Upon cooling to ambient temperature, a solid precipitate was collected by filtration and washed with a 1:1 EtOH/water mixture followed by

Et<sub>2</sub>O. The solids were dried under high vacuum to give Zn((E)-2-(2-(1-(pyridin-2-yl)ethylidene)hydrazinyl)benzo[d]thiazole)<sub>2</sub> (**Zn-2**) (64.6 mg, 0.108 mmol, 77%) as an orange solid. <sup>1</sup>H NMR (500 MHz, DMSO-*d*<sub>6</sub>) δ 7.88 (td, *J* = 5.8, 5.1, 3.5 Hz, 4H), 7.82 (dd, *J* = 8.5, 1.1 Hz, 2H), 7.45 (dd, *J* = 7.8, 1.2 Hz, 2H), 7.26 (ddd, *J* = 7.4, 5.2, 1.1 Hz, 2H), 6.95 (td, *J* = 7.7, 7.3, 1.2 Hz, 2H), 6.75 (td, *J* = 7.6, 1.2 Hz, 2H), 6.60 (d, *J* = 8.0 Hz, 2H), 2.63 (s, 6H). Slow evaporation of [Zn(Cl)<sub>2</sub>] from THF afforded orange crystals that were suitable for X-ray crystallography. HRMS (MALDI) (*m/z*): [M + H<sup>+</sup>] calcd for C<sub>28</sub>H<sub>22</sub>N<sub>8</sub>S<sub>2</sub>Zn + H<sup>+</sup>, 599.07500; found, 599.0773.

**2,2'-((2-Ethoxy-2-oxoethyl)azanediyl)diacetic acid (NTA-MEE).** To a suspension of nitrilotriacetic acid (1.91 g, 10 mmol, 1 equiv) in DMF (4 mL) was added acetic anhydride (1.13 mL, 12 mmol, 1.2 equiv) and pyridine (0.1 mL). The reaction mixture was heated to 70 °C and stirred for 18 h. The reaction vessel was equipped with a short-path distillation apparatus, and the volatiles were removed by distillation. EtOH (0.6 mL, 0.46 g, 10 mmol, 1 equiv) was added to the remaining mother liquor. The solution was sonicated for 30 min and diluted with water. A solid precipitate was removed by filtration, and the aqueous filtrate was extracted 3× with EtOAc. The organic layers were discarded, and the aqueous layer was retained. The water was removed azeotropically with additional EtOH by rotary evaporation to give 2,2'-((2-ethoxy-2-oxoethyl)azanediyl)diacetic acid (**NTA-MEE**) as a hygroscopic brown foam (0.232 mgs, 1.06 mmol, 11%). <sup>1</sup>H NMR (500 MHz, DMSO-*d*<sub>6</sub>): δ 12.36 (bs, 2H), 4.07 (q, *J* = 7.1 Hz, 2H), 3.56 (s, 2H), 3.50 (s, 4H), 1.18 (t, *J* = 7.1 Hz, 3H).

**Bis(2-ethoxy-2-oxoethyl)glycine (NTA-DEE).** To a solution of diethyl 2,2'-azanediyl diacetate (1.9 mL, 10.6 mmol, 2 equiv) in dioxane (6.5 mL) was added 2-bromoacetic acid (0.38 mL, 5.3 mmol, 1 equiv). After heating overnight at 60 °C, the crude reaction was concentrated under reduced pressure. The residual oil was dissolved in DCM and washed in succession 1× with NaHCO<sub>3</sub>(sat, aq), 1× with water, and 1× with brine. The organic was dried over Na<sub>2</sub>SO<sub>4</sub>, filtered, concentrated, and dried under high vacuum to give the title compound bis(2-ethoxy-2-oxoethyl)glycine (**NTA-DEE**) as a brown oil. <sup>1</sup>H NMR (500 MHz, DMSO-*d*<sub>6</sub>): δ 4.04 (q, *J* = 7.1 Hz, 4H), 3.55 (s, 4H), 3.47 (s, 2H), 1.16 (t, *J* = 7.1 Hz, 6H).

**K<sub>Zn</sub> and K<sub>Cu</sub> Measurements.** K<sub>d</sub> measurements of zinc and copper were performed, as described previously.<sup>36</sup>

**Zn<sup>2+</sup>-K<sub>d</sub> Measurements by Competition.** The compounds in 50 mM Tris (pH 7.2) and 150 mM NaCl (compound concentrations: 2-fold serial dilution from 10,000 to 4.9 nM) were incubated with 30 nM ZnCl<sub>2</sub> + 30 nM FluoZin-3 or RhodZin-3 reporter at room temperature for 60 min in Costar black polystyrene 96-well plates (Corning Inc., Corning, NY), and the fluorescence was measured using a SpectraMax i3x plate reader (λ<sub>ex</sub> = 500 nm; λ<sub>em</sub> = 540 nm) (Molecular Devices, LLC, Sunnyvale, CA). The data were plotted on a log axis and fit to a sigmoid to measure IC<sub>50</sub>

$$y = \frac{A}{1 + e^{-(x-x_0)/b}} \quad (1)$$

where *y* is the measured fluorescence, *A* is the curve amplitude, *x* is log[compound], *x*<sub>0</sub> is the log IC<sub>50</sub>, and *b* is an empirical steepness parameter. That IC<sub>50</sub> was then used in the Munson–Robard solution to the Cheng–Prussif equation to calculate K<sub>d</sub>

$$K_i = \frac{IC_{50}}{1 + \frac{L_T(y_0 + 2)}{2K_d(y_0 + 1)} + y_0} - K_d \frac{y_0}{y_0 + 2} \quad (2)$$

where K<sub>i</sub> is the dissociation constant of the DBD, L<sub>T</sub> is the total concentration of the reporter, K<sub>d</sub> is the dissociation constant of the reporter for Zn<sup>2+</sup> (15 and 65 nM for FluoZin-3 and RhodZin-3, respectively, per manufacturer), and y<sub>0</sub> is the ratio of bound reporter to free reporter in the absence of the study compound (e.g., 15 nM/15 nM in the case of FluoZin-3). Curve fitting was done in SigmaPlot 13.0.

FluoZin-3 and RhodZin-3 were used interchangeably, depending on commercial availability.

**Cu<sup>2+</sup>-K<sub>d</sub> Measurements by Competition.** Compound (6 μM) and CuSO<sub>4</sub> (8 μM) in 150 mM NaCl and 20 mM Tris (pH 7.2) were incubated with EGTA (10<sup>-1</sup>–10<sup>-7</sup> M, 1.8-fold dilution series) at room temperature in a transparent, flat-bottom 96-well plate. Absorbance spectra from 200 to 550 nm were acquired after using a SpectraMax i3x plate reader. The spectra were blank-subtracted using a matched dilution of EGTA in buffer, and the absorbance maximum of the compound with Cu<sup>2+</sup> was plotted versus EGTA concentration. These data were fit to a sigmoid, and the IC<sub>50</sub> was used to calculate the K<sub>Cu</sub> of the compound as described above. The K<sub>Cu</sub> of EGTA under the experimental conditions was determined using WinMAXC (C. Patton, Stanford University).

**Oxidative Stress Detection.** The ROS signal was measured using CellROX Green reagent (Thermo Fisher Scientific, Carlsbad, CA) following manufacturer's protocol. Briefly, H1299 cells were seeded at 2.2 × 10<sup>5</sup> per well in 12-well plates overnight and treated with 0.75 μM corresponding compound for 24 h. CellROX Green (5 μM) was added to each well and incubated for 30 min. The cells were harvested, and the fluorescence signal was measured using a Cytomics FC500 flow cytometer. The p53 null cells were used to minimize any p53 effects.

**Cell Growth Inhibition Assay.** The cell growth inhibition assay was performed by MTS (Promega) or Calcein AM assay (Trevigen), as described previously.<sup>36</sup> Briefly, 5000 cells per well were cultured in a 96-well plate to reach the 50% confluence on the second day when treated with serial dilutions of the compounds. Growth was measured either by the MTS reagent or Calcein AM assay and Tecan plate reader instrument (Tecan) after incubation for 3 days. Statistical significance of the data, obtained from three independent experiments, each with triplicates, was calculated with Student's *t* test.

**Immunofluorescence Staining.** Immunofluorescence staining was performed, as described previously.<sup>8</sup> In brief, cells were grown on coverslips followed by various treatments. The coverslips were fixed with 4% paraformaldehyde for 10 min and then permeabilized with 0.5% Triton X-100 for 5 min. The conformation of the mutant and WT p53 proteins was recognized specifically by the antibodies PAB1620 (1:50, recognizing wild-type conformation) and PAB240 (1:400, recognizing misfolded/unfolded conformation) stained overnight, respectively. The secondary antibody, goat antimouse IgG, was incubated for 40 min. PAB1620 and PAB240 were purchased from EMD Chemicals.

**Efflux Analysis.** Caco-2 assays were performed by Sai Life Sciences (Hinjewadi, India). Briefly, Caco-2 cells were seeded in 24-well Millicell plates and incubated for 21 days. For A–B transport, the candidate compounds and loperamide were added to the apical side. For B–A transport, the candidate compounds and loperamide were added to the basal side. At 0, 15, 30, 60, and 90 min, aliquots of 50 μL were collected from the receiver compartment for determination of the candidate compound concentrations by LC–MS/MS.

**Mouse Experiments.** Mice are housed and treated according to guidelines, and all the mouse experiments are done with the approval of Institutional Animal Care and Use Committee (IACUC) of Rutgers University. The nude mice NCr nu/nu are purchased from Taconic. The acute toxicity and efficacy assays were performed, as described previously.<sup>36</sup> Briefly, for the maximum tolerated dose assays, 8–12 week old mice (5 mice per dose) were administered by intraperitoneal injection (ip) once for acute test and health, behavior, and body weight were monitored. The survival times of these groups were shown in Kaplan–Meier survival curves with the log-rank test. Xenograft tumor assays were derived from the human tumor cell lines, TOV-112D (5 × 10<sup>6</sup> cells/tumor site/mouse) and MDA-MB-468 (6 × 10<sup>6</sup> cells/tumor site/mouse). Tumor dimensions were measured every other day, and their volumes were calculated by length (*L*) and width (*W*) using the formula: volume = *L* × *W*<sup>2</sup> × π/6. Tumors (five per group) were allowed to grow to 50 mm<sup>3</sup> prior to daily administration of each compound administered ip at the doses detailed in the text.

**Hydrolytic Stability Studies.** A detailed procedure is reported in the Supporting Information.



**Statistical Methods.** The data were analyzed by Student's *t* test with an overall significance level of  $p < 0.05$ . *p* values were described in each figure and in the text. \* $p < 0.05$ , \*\* $p < 0.01$ , and \*\*\* $p < 0.001$ .

## ■ ASSOCIATED CONTENT

### Supporting Information

The Supporting Information is available free of charge at <https://pubs.acs.org/doi/10.1021/acs.jmedchem.0c01360>.

Suppl. Figure S1, S2, and S3; Hydrolytic Stability Studies of ZMC1 and C85; HPLC traces (PDF)  
Molecular formula strings of all compounds (CSV)  
X-ray crystallographic data of Zn-1 (CIF)  
X-ray crystallographic data of Zn-2 (CIF)

## ■ AUTHOR INFORMATION

### Corresponding Author

Darren R. Carpizo – Division of Surgical Oncology, Department of Surgery, University of Rochester Medical Center, Rochester, New York 14642, United States; Wilmot Cancer Center, University of Rochester, Rochester, New York 14642, United States; Email: [darren.carpizo@urmc.rochester.edu](mailto:darren.carpizo@urmc.rochester.edu)

### Authors

John A. Gilleran – Rutgers Molecular Design and Synthesis, Office of Research and Economic Development, Piscataway, New Jersey 08854, United States  
Xin Yu – Program of Surgical Oncology, Rutgers Cancer Institute of New Jersey and Department of Surgery, Robert Wood Johnson Medical School, Rutgers University, New Brunswick, New Jersey 08901, United States  
Alan J. Blayney – Department of Biochemistry and Molecular Biology, SUNY Upstate Medical University, Syracuse, New York 13210, United States  
Anthony F. Bencivenga – Rutgers Molecular Design and Synthesis, Office of Research and Economic Development, Piscataway, New Jersey 08854, United States  
Bing Na – Program of Surgical Oncology, Rutgers Cancer Institute of New Jersey and Department of Surgery, Robert Wood Johnson Medical School, Rutgers University, New Brunswick, New Jersey 08901, United States  
David J. Augeri – Rutgers Molecular Design and Synthesis, Office of Research and Economic Development, Piscataway, New Jersey 08854, United States  
Adam R. Blanden – Department of Biochemistry and Molecular Biology, SUNY Upstate Medical University, Syracuse, New York 13210, United States  
S. David Kimball – Rutgers Molecular Design and Synthesis, Office of Research and Economic Development, Piscataway, New Jersey 08854, United States  
Stewart N. Loh – Department of Biochemistry and Molecular Biology, SUNY Upstate Medical University, Syracuse, New York 13210, United States  
Jacques Y. Roberge – Rutgers Molecular Design and Synthesis, Office of Research and Economic Development, Piscataway, New Jersey 08854, United States; [orcid.org/0000-0002-7810-4139](https://orcid.org/0000-0002-7810-4139)

Complete contact information is available at:

<https://pubs.acs.org/doi/10.1021/acs.jmedchem.0c01360>

### Author Contributions

<sup>†</sup>J.G., X.Y., and A.J.B. contributed equally to this work.

### Author Contributions

<sup>‡</sup>S.N.L., J.Y.R., and D.R.C. are co-senior authors.

### Funding

This work was supported by grants from the NIH (R01 CA200800 and K08 CA172676), the Breast Cancer Research Foundation (to D.R.C.), and the NIH (F30GM113299) (to A.R.B.).

### Notes

The authors declare the following competing financial interest(s): D.R.C. is the founders of Z53 Therapeutics, Inc., a company that aims to develop p53 mutant reactivators such as zinc metallochaperons into therapeutic agents for the treatment of cancer and other diseases. J.Y.R. is a paid consultant, and own options, of Pacylex Pharmaceuticals, a company developing PCLX-001 for oncology targets. No potential conflicts of interest were disclosed by the other authors.

## ■ ABBREVIATIONS

ATCC, American Type Culture Collection; Caco-2, human colorectal adenocarcinoma cells; CDL, curved desolvation line; DBD, DNA binding domain; DEE, diethyl ester; DMEM, Dulbecco's modified Eagle's medium; EGTA, egtazic acid; FBS, fetal bovine serum; Gy, gray; Hex, *n*-hexanes; IACUC, Institutional Animal Care and Use Committee; MEE, monoethyl ester; MsCl, methanesulfonyl chloride; MTS, 3-(4,5-dimethylthiazol-2-yl)-5-(3-carboxymethoxyphenyl)-2-(4-sulfophenyl)-2H-tetrazolium; NTA, nitrilotriacetic acid; Pab, p53 antibody; PBS, phosphate-buffered saline; PTM, post-translational modification; RR, ribonucleotide reductase; SGF, simulated gastric fluid; TEA, triethylamine; TSC, thiosemicarbazone; ZMC, zinc metallochaperone

## ■ REFERENCES

- (1) Blanden, A. R.; Yu, X.; Loh, S. N.; Levine, A. J.; Carpizo, D. R. Reactivating mutant p53 using small molecules as zinc metallochaperones: awakening a sleeping giant in cancer. *Drug Discovery Today* **2015**, *20*, 1391–1397.
- (2) Yu, X.; Carpizo, D. R. Flipping the "switch" on mutant p53 by zinc metallochaperones: how a brief pulse of zinc can reactivate mutant p53 to kill cancer. *Oncotarget* **2019**, *10*, 918–919.
- (3) Cho, Y.; Gorina, S.; Jeffrey, P. D.; Pavletich, N. P. Crystal structure of a p53 tumor suppressor-DNA complex: understanding tumorigenic mutations. *Science* **1994**, *265*, 346–355.
- (4) Hainaut, P.; Milner, J. A structural role for metal ions in the "wild-type" conformation of the tumor suppressor protein p53. *Cancer Res.* **1993**, *53*, 1739–1742.
- (5) Méplan, C.; Richard, M.-J.; Hainaut, P. Metalloregulation of the tumor suppressor protein p53: zinc mediates the reactivation of p53 after exposure to metal chelators in vitro and in intact cells. *Oncogene* **2000**, *19*, 5227–5236.
- (6) Blanden, A. R.; Yu, X.; Wolfe, A. J.; Gilleran, J. A.; Augeri, D. J.; O'Dell, R. S.; Olson, E. C.; Kimball, S. D.; Emge, T. J.; Movileanu, L.; Carpizo, D. R.; Loh, S. N. Synthetic metallochaperone ZMC1 rescues mutant p53 conformation by transporting zinc into cells as an ionophore. *Mol. Pharmacol.* **2015**, *87*, 825–831.
- (7) Yu, X.; Blanden, A.; Tsang, A. T.; Zaman, S.; Liu, Y.; Gilleran, J.; Bencivenga, A. F.; Kimball, S. D.; Loh, S. N.; Carpizo, D. R. Thiosemicarbazones functioning as zinc metallochaperones to reactivate mutant p53. *Mol. Pharmacol.* **2017**, *91*, 567–575.
- (8) Yu, X.; Vazquez, A.; Levine, A. J.; Carpizo, D. R. Allele-specific p53 mutant reactivation. *Cancer Cell* **2012**, *21*, 614–625.
- (9) Na, B.; Yu, X.; Withers, T.; Gilleran, J.; Yao, M.; Foo, T. K.; Chen, C.; Moore, D.; Lin, Y.; Kimball, S. D.; Xia, B.; Ganesan, S.; Carpizo, D. R. Therapeutic targeting of BRCA1 and TP53 mutant

breast cancer through mutant p53 reactivation. *NPJ Breast Cancer* **2019**, *5*, 14.

(10) Yu, X.; Kogan, S.; Chen, Y.; Tsang, A. T.; Withers, T.; Lin, H.; Gilleran, J.; Buckley, B.; Moore, D.; Bertino, J.; Chan, C.; Kimball, S. D.; Loh, S. N.; Carpizo, D. R. Zinc metallochaperones reactivate mutant p53 using an ON/OFF switch mechanism: A new paradigm in cancer therapeutics. *Clin Cancer Res* **2018**, *24*, 4505–4517.

(11) Agrawal, K. C.; Sartorelli, A. C. 7 The Chemistry and Biological Activity of  $\alpha$ -(N)-Heterocyclic Carboxaldehyde Thiosemicarbazones. *Prog. Med. Chem.* **1978**, *15*, 321–356.

(12) Yu, Y.; Kalinowski, D. S.; Kovacevic, Z.; Siafakas, A. R.; Jansson, P. J.; Stefani, C.; Lovejoy, D. B.; Sharpe, P. C.; Bernhardt, P. V.; Richardson, D. R. Thiosemicarbazones from the old to new: iron chelators that are more than just ribonucleotide reductase inhibitors. *J. Med. Chem.* **2009**, *52*, 5271–5294.

(13) Shimada, K.; Reznik, E.; Stokes, M. E.; Krishnamoorthy, L.; Bos, P. H.; Song, Y.; Quartararo, C. E.; Pagano, N. C.; Carpizo, D. R.; de Carvalho, A. C.; Lo, D. C.; Stockwell, B. R. Copper-binding small molecule induces oxidative stress and cell-cycle arrest in glioblastoma-patient-derived cells. *Cell Chem. Biol.* **2018**, *25*, 585–594.e7 e7.

(14) Yu, X.; Blanden, A. R.; Narayanan, S.; Jayakumar, L.; Lubin, D.; Augeri, D.; Kimball, S. D.; Loh, S. N.; Carpizo, D. R. Small molecule restoration of wildtype structure and function of mutant p53 using a novel zinc-metallochaperone based mechanism. *Oncotarget* **2014**, *5*, 8879–8892.

(15) Meek, D. W.; Anderson, C. W. Posttranslational modification of p53: cooperative integrators of function. *Cold Spring Harbor Perspect. Biol.* **2009**, *1*, a000950.

(16) Blindauer, C. A.; Harvey, I.; Bunyan, K. E.; Stewart, A. J.; Sleep, D.; Harrison, D. J.; Berezenko, S.; Sadler, P. J. Structure, properties, and engineering of the major zinc binding site on human albumin. *J. Biol. Chem.* **2009**, *284*, 23116–23124.

(17) Masuoka, J.; Hegenauer, J.; Van Dyke, B. R.; Saltman, P. Intrinsic stoichiometric equilibrium constants for the binding of zinc(II) and copper(II) to the high affinity site of serum albumin. *J. Biol. Chem.* **1993**, *268*, 21533–21537.

(18) Lu, J.; Stewart, A. J.; Sadler, P. J.; Pinheiro, T. J. T.; Blindauer, C. A. Albumin as a zinc carrier: properties of its high-affinity zinc-binding site. *Biochem. Soc. Trans.* **2008**, *36*, 1317–1321.

(19) Blanden, A. R.; Yu, X.; Blayney, A. J.; Demas, C.; Ha, J. H.; Liu, Y.; Withers, T.; Carpizo, D. R.; Loh, S. N. Zinc shapes the folding landscape of p53 and establishes a pathway for reactivating structurally diverse cancer mutants. *Elife* **2020**, *9*, No. e61487.

(20) Stacy, A. E.; Palanimuthu, D.; Bernhardt, P. V.; Kalinowski, D. S.; Jansson, P. J.; Richardson, D. R. Structure-activity relationships of di-2-pyridylketone, 2-benzoylpyridine, and 2-acetylpyridine thiosemicarbazones for overcoming pgp-mediated drug resistance. *J. Med. Chem.* **2016**, *59*, 8601–8620.

(21) Lökön, M.; Tshepelevitsh, S.; Heering, A.; Plieger, P. G.; Vianello, R.; Leito, I. On the basicity of conjugated nitrogen heterocycles in different media. *Eur. J. Org. Chem.* **2017**, *2017*, 4475–4489.

(22) Easmon, J.; Heinisch, G.; Pürstinger, G.; Langer, T.; Österreicher, J. K.; Grunicke, H. H.; Hofmann, J. Azinyl and diazanyl hydrazones derived from aryl N-heteroaryl ketones: synthesis and antiproliferative activity. *J. Med. Chem.* **1997**, *40*, 4420–4425.

(23) ChemAxon; <https://chemicalize.com/welcome/chemical-calculations-and-predictions>. (accessed Apr 27, 2020).

(24) Pelivan, K.; Frensemeier, L. M.; Karst, U.; Koellensperger, G.; Heffeter, P.; Keppler, B. K.; Kowol, C. R. Comparison of metabolic pathways of different  $\alpha$ -N-heterocyclic thiosemicarbazones. *Anal. Bioanal. Chem.* **2018**, *410*, 2343–2361.

(25) Schaper, K. J.; Seydel, J. K.; Rosenfeld, M.; Kazda, J. Development of inhibitors of mycobacterial ribonucleotide reductase. *Lepr. Rev.* **1986**, *57*, 254–264.

(26) Easmon, J.; Pürstinger, G.; Thies, K.-S.; Heinisch, G.; Hofmann, J. Synthesis, structure-activity relationships, and antitumor studies of 2-benzoxazolyl hydrazones derived from  $\alpha$ -(N)-acyl heteroaromatics. *J. Med. Chem.* **2006**, *49*, 6343–6350.

(27) Easmon, J.; Puerstinger, G.; Roth, T.; Fiebig, H. H.; Jenny, M.; Jaeger, W.; Heinisch, G.; Hofmann, J. 2-benzoxazolyl and 2-benzimidazolyl hydrazones derived from 2-acetylpyridine: a novel class of antitumor agents. *Int. J. Cancer* **2001**, *94*, 89–96.

(28) Eurofins; <https://www.eurofinsdiscoveryservices.com/catalogmanagement/viewitem/SafetyScreen44-Panel-Cerep/P270>. (accessed Apr 9, 2020).

(29) Ghose, A. K.; Viswanadhan, V. N.; Wendoloski, J. J. Prediction of hydrophobic (lipophilic) properties of small organic molecules using fragmental methods: An analysis of ALOGP and CLOGP methods. *J. Phys. Chem. A* **1998**, *102*, 3762–3772.

(30) Prasanna, S.; Doerksen, R. J. Topological polar surface area: a useful descriptor in 2D-QSAR. *Curr. Med. Chem.* **2009**, *16*, 21–41.

(31) Muehlbacher, M.; Spitzer, G. M.; Liedl, K. R.; Kornhuber, J. Qualitative prediction of blood-brain barrier permeability on a large and refined dataset. *J. Comput.-Aided Mol. Des.* **2011**, *25*, 1095–1106.

(32) Kourounakis, A. P.; Xanthopoulos, D.; Tzara, A. Morpholine as a privileged structure: A review on the medicinal chemistry and pharmacological activity of morpholine containing bioactive molecules. *Med. Res. Rev.* **2020**, *40*, 709–752.

(33) Kerns, E. H.; Di, L. hERG Blocking. In *Drug-Like Properties: Concepts, Structure Design And Methods, From Adme To Toxicity Optimization*; Academic Press: San Diego, 2008, p 209–214.

(34) Lowe, S. W.; Bodis, S.; McClatchey, A.; Remington, L.; Ruley, H. E.; Fisher, D. E.; Housman, D. E.; Jacks, T. p53 status and the efficacy of cancer therapy in vivo. *Science* **1994**, *266*, 807–810.

(35) Lowe, S. W.; Ruley, H. E.; Jacks, T.; Housman, D. E. p53-dependent apoptosis modulates the cytotoxicity of anticancer agents. *Cell* **1993**, *74*, 957–967.

(36) Zaman, S.; Yu, X.; Bencivenga, A. F.; Blanden, A. R.; Liu, Y.; Withers, T.; Na, B.; Blayney, A. J.; Gilleran, J.; Boothman, D. A.; Loh, S. N.; Kimball, S. D.; Carpizo, D. R. Combinatorial therapy of zinc metallochaperones with mutant p53 reactivation and diminished copper binding. *Mol. Cancer Ther.* **2019**, *18*, 1355–1365.

(37) Banci, L.; Bertini, I.; Ciofi-Baffoni, S.; Kozyreva, T.; Zovo, K.; Palumaa, P. Affinity gradients drive copper to cellular destinations. *Nature* **2010**, *465*, 645–648.

(38) Toth, B. Synthetic and naturally occurring hydrazines as possible cancer causative agents. *Cancer Res.* **1975**, *35*, 3693–3697.

(39) Lagrange, E.; Vernoux, J. P. Warning on false or true morels and button mushrooms with potential toxicity linked to hydrazinic toxins: An update. *Toxins (Basel)* **2020**, *12*, 482.

(40) Drugbank; <https://www.drugbank.ca/>. (accessed Apr 28, 2020).

(41) Cramer, J.; Krimmer, S. G.; Heine, A.; Klebe, G. Paying the price of desolvation in solvent-exposed protein pockets: Impact of distal solubilizing groups on affinity and binding thermodynamics in a series of thermolysin inhibitors. *J. Med. Chem.* **2017**, *60*, 5791–5799.

(42) Chandler, P.; Kochupurakkal, B. S.; Alam, S.; Richardson, A. L.; Soybel, D. I.; Kelleher, S. L. Subtype-specific accumulation of intracellular zinc pools is associated with the malignant phenotype in breast cancer. *Mol Cancer* **2016**, *15*, 2.

## ■ NOTE ADDED AFTER ASAP PUBLICATION

After this paper was published ASAP on February 4, 2021, spelling errors were corrected in a suffix used throughout the paper (-zoyl to -zoyl). The corrected version was reposted February 8, 2021.